Diffractive and exclusive measurements with the CMS experiment

Gustavo G. da Silveira
gustavo.silveira@cern.ch

Centre for Cosmology, Particle Physics and Phenomenology (CP3)
Universite catholique de Louvain (UCL), Belgium

on behalf of the CMS Collaboration

Outline

- CMS detector and capabilities for forward physics;
- Diffractive & Exclusive processes in CMS;
- Measurement of diffractive dissociation cross sections in CMS;
  - Single diffraction (forward gap + no CASTOR);
  - Double diffraction (forward gap + CASTOR) – low & high masses;
  - Double diffraction (central gap) – high masses.
- Exclusive production of massive electroweak-boson pairs;
  - Measurement of exclusive $\gamma\gamma \to \mu^+\mu^-$ at large masses – control;
  - Search for exclusive $\gamma\gamma \to W^+W^-$ production;
  - Limits on anomalous quartic gauge couplings.

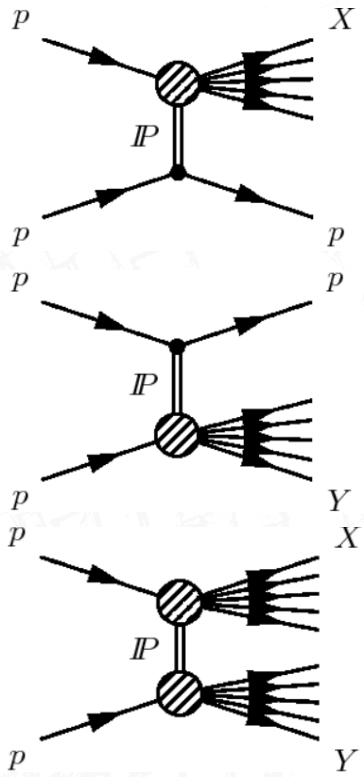

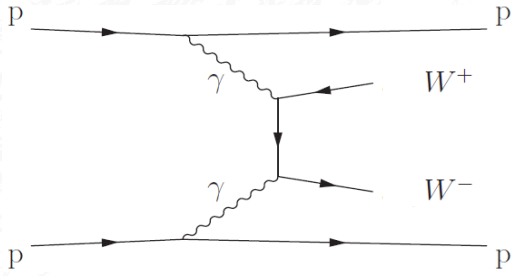

Large Hadron Collider

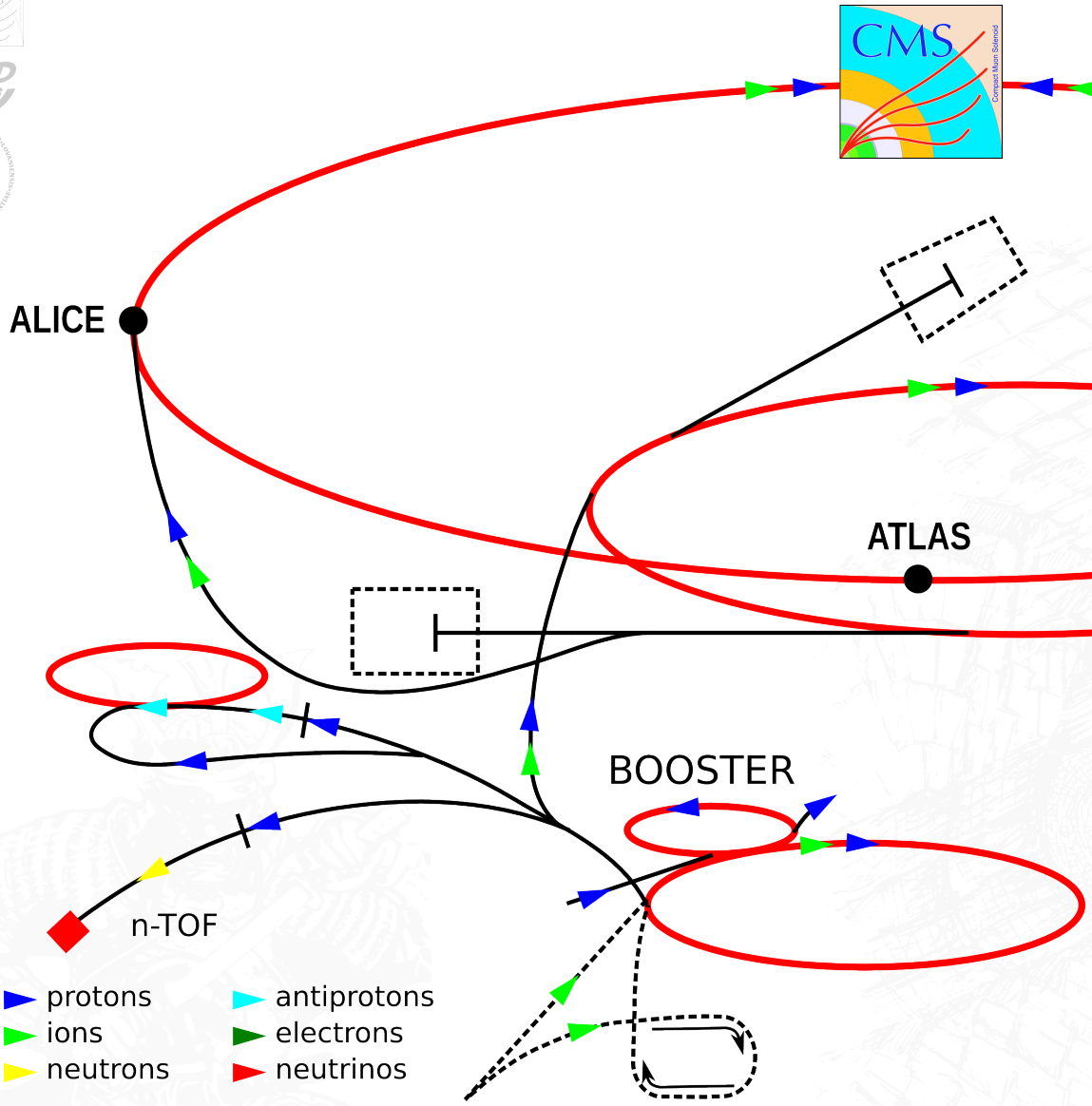

2010	E_{pp} = 7 TeV L = 44.22 pb^{-1}	E_{PbPb} = 2.76 TeV L = 7.00 μb^{-1}
2011	E_{pp} = 7 TeV L = 6.13 fb^{-1}	E_{PbPb} = 2.76 TeV L = 157.57 μb^{-1}
2012	E_{pp} = 8 TeV L = 23.30 fb^{-1}	-
2013	E_{pp} = 2.76 TeV L = 5.51 pb^{-1}	E_{pPb} = 5.02 TeV L = 35.50 nb^{-1}
2015	E_{pp} = 13 TeV L ~ 50.00 fb^{-1}	(expected)

The CMS experiment

Total weight : 14k tonnes
Overall diameter : 15.0 m
Overall length : 28.7 m
Magnetic field : 3.8 T

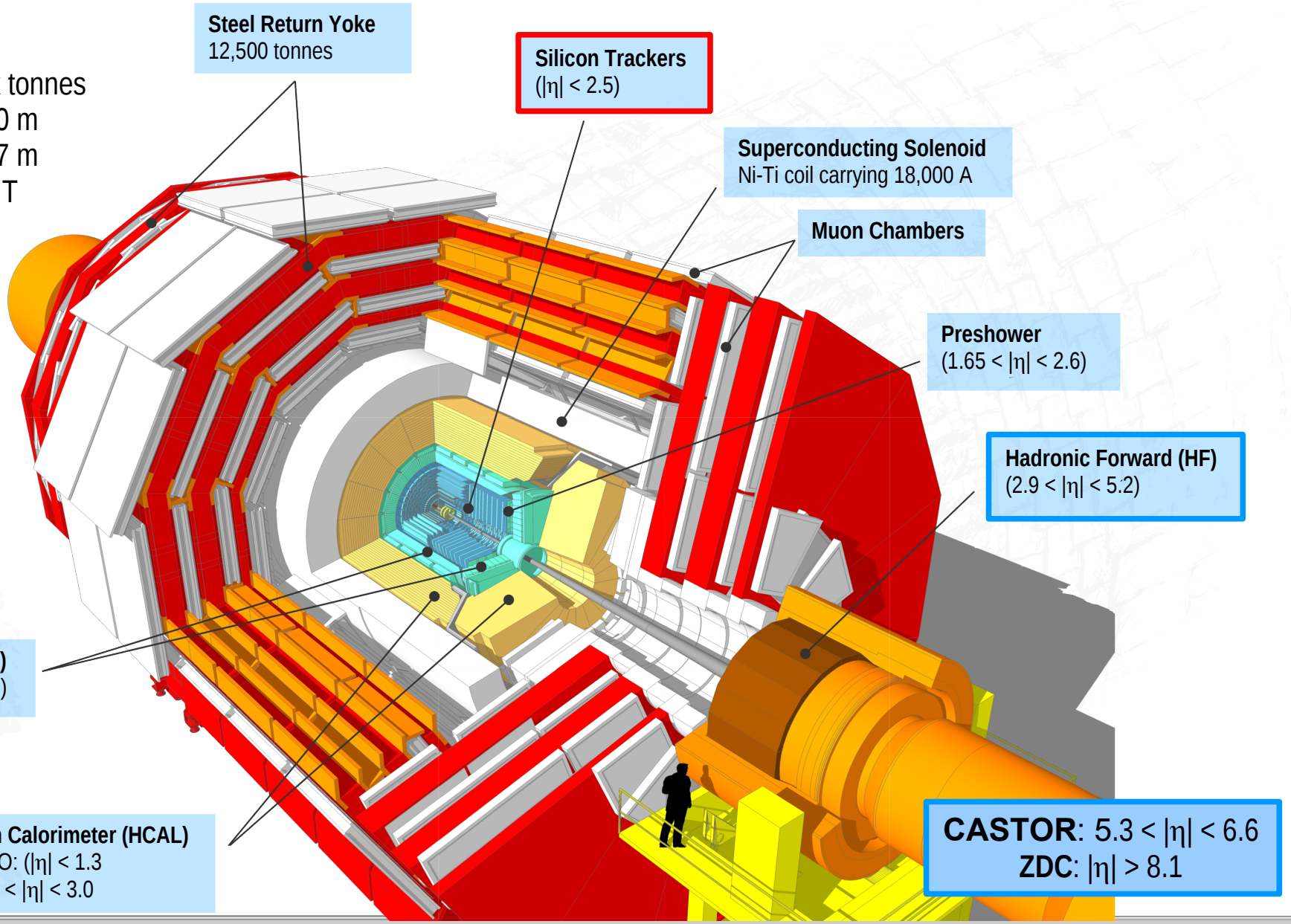

Outline

- CMS detector and capabilities for forward physics;
- Diffractive & Exclusive processes in CMS;
- Measurement of diffractive dissociation cross sections in CMS;
  - Single diffraction (forward gap + no CASTOR);
  - Double diffraction (forward gap + CASTOR) – low & high masses;
  - Double diffraction (central gap) – high masses.
- Exclusive production of massive electroweak-boson pairs;
  - Measurement of exclusive gg → m+m- at large masses – control;
  - Search for exclusive gg → W+W- production;
  - Limits on anomalous quartic gauge couplings.

Diffractive processes in CMS

- Diffractive processes are characterized by three different topologies, which can be summarized as follows:

Non-Diffractive	$pp \rightarrow X$
Single diffraction	$pp \rightarrow p + LRG + Y$
Double diffraction	$pp \rightarrow X + LRG + Y$
Central diffraction	$pp \rightarrow p + LRG + X + LRG + p$

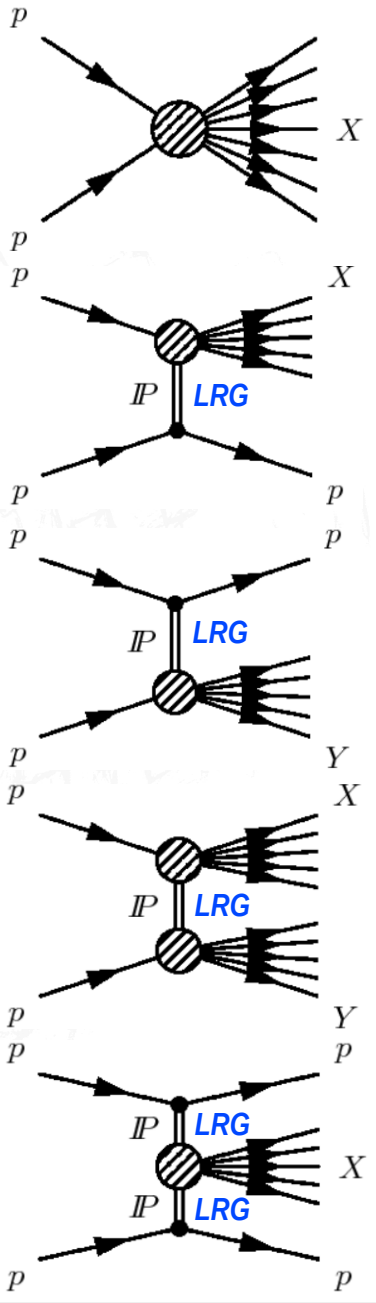

- ***L**arge **R**apidity **G**aps*: gap with no hadronic activity, which is the main experimental signature to measure diffractive processes;

- The interaction is medaited by the exchange of a **Pomeron** (*IP*): color-singlet with vacuum quantum numbers;

- Measurements of diffractive cross sections are essential to test|improve the theoretical predictions – usually models based on the **Regge theory**:
  - 3*IP* coupling, flux renormalization, factorization breaking, etc.

Exclusive processes in CMS

- The exclusive production of light and heavy pairs is represented by:

$$pp \rightarrow p^{(*)} + (\gamma\gamma, \ell^+\ell^-, \mathrm{W}^+\mathrm{W}^-) + p^{(*)}$$

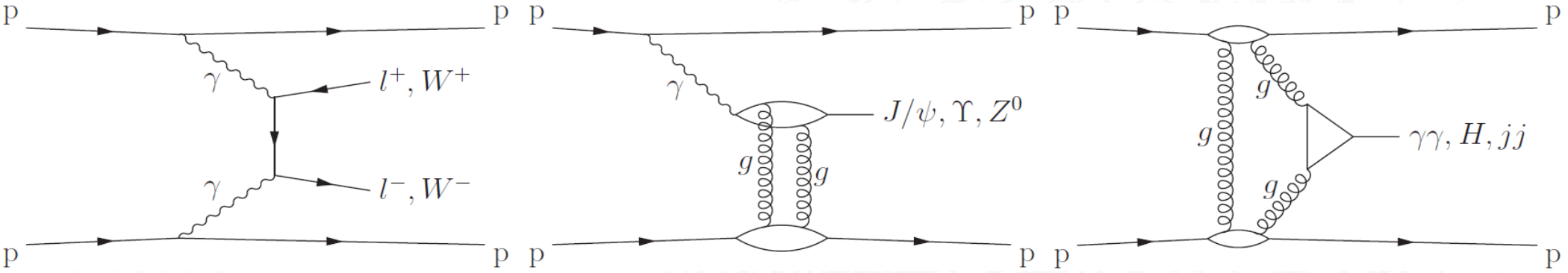

- Intact protons in the final states, however also accounting for **proton dissociation p^***;
- **No other particles** observed in the central detector apart of the signal;

$\gamma\gamma$	tests theoretical predictions for **exclusive Higgs production** and to measure **gluon density at small-x**;
$\ell^+\ell^-$	comparison to precision QED predictions and to study of **proton dissociation**;
$\mathrm{W}^+\mathrm{W}^-$	study of exclusive processes at high mass and constraint of **anomalous couplings**.

Outline

- CMS detector and capabilities for forward physics;
- Diffractive & Exclusive processes in CMS;
- Measurement of diffractive dissociation cross sections in CMS;
  - Single diffraction (forward gap + no CASTOR);
  - Double diffraction (forward gap + CASTOR) – low & high masses;
  - Double diffraction (central gap) – high masses.
- Exclusive production of massive electroweak-boson pairs;
  - Measurement of exclusive $\gamma\gamma \to \mu^+\mu^-$ at large masses – control;
  - Search for exclusive $\gamma\gamma \to W^+W^-$ production;
  - Limits on anomalous quartic gauge couplings.

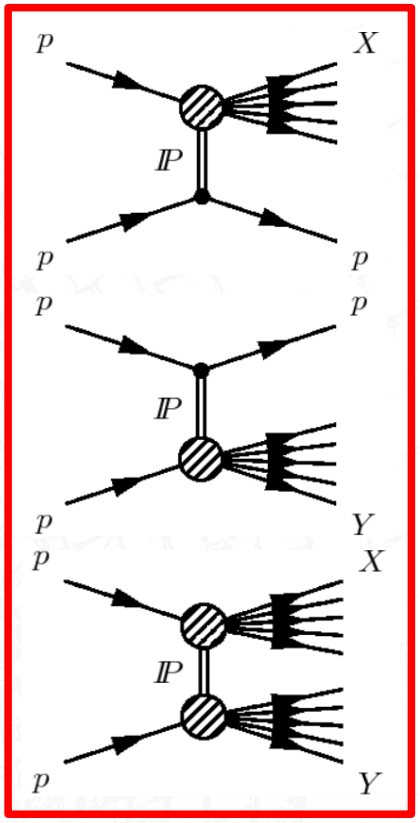

CMS PAS FSQ-12-005

Event selection

- Low pU data collected by CMS at E_{pp} of 7 TeV in 2010:
  - CASTOR calorimeter only: **16.2 μb^{-1}**;
  - $\langle N_{inel,pp} \rangle$/BX ≡ **$\mu$ = 0.14**.

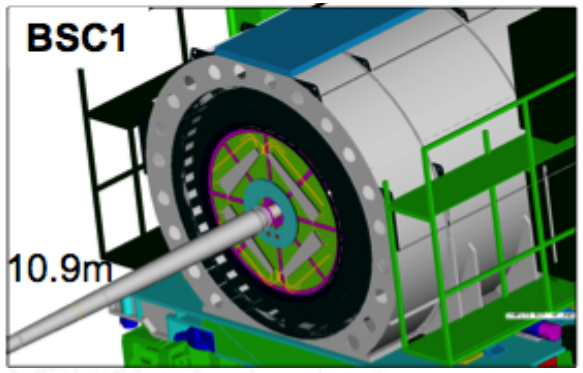

- The online selection considers the combined information from different components:
  - Signal in both *Beam Pick-up Timing Experiment* (BPTX);
  - Signal in any of the *Beam Scintillator Counters* (BSC);
  - Combined result: **bunch crossing at the IP + activity in the central detector**.

- An offline requirements are employed to clean the signal:
  - **>25%** of high-quality tracks in events with 10+ reco tracks;
  - Reject **beam-halo events**;
  - Events coinsistent with contamination from **noise in HCAL** are discarded.

No vertex requirement

↓

High acceptance for $M_X \lesssim 100$ GeV

Definition of experimental survey

- The topologies can be defined based on the position of the LRG in the **central dectetor**;
- Forward gap is defined in terms of the **highest** (η_{max}) or **lowest** (η_{min}) pseudorapidity of PF object in the central detector for **single dissociative** events;
  - SD1: gap at η+ region;
  - SD2: gap at η− region.
- **Double dissociative** events: central gap is defined in terms of the closest-to-zero η of PF object on the **positive** (η^0_{max}) or **negative** (η^0_{min}) η-side of the central detector;

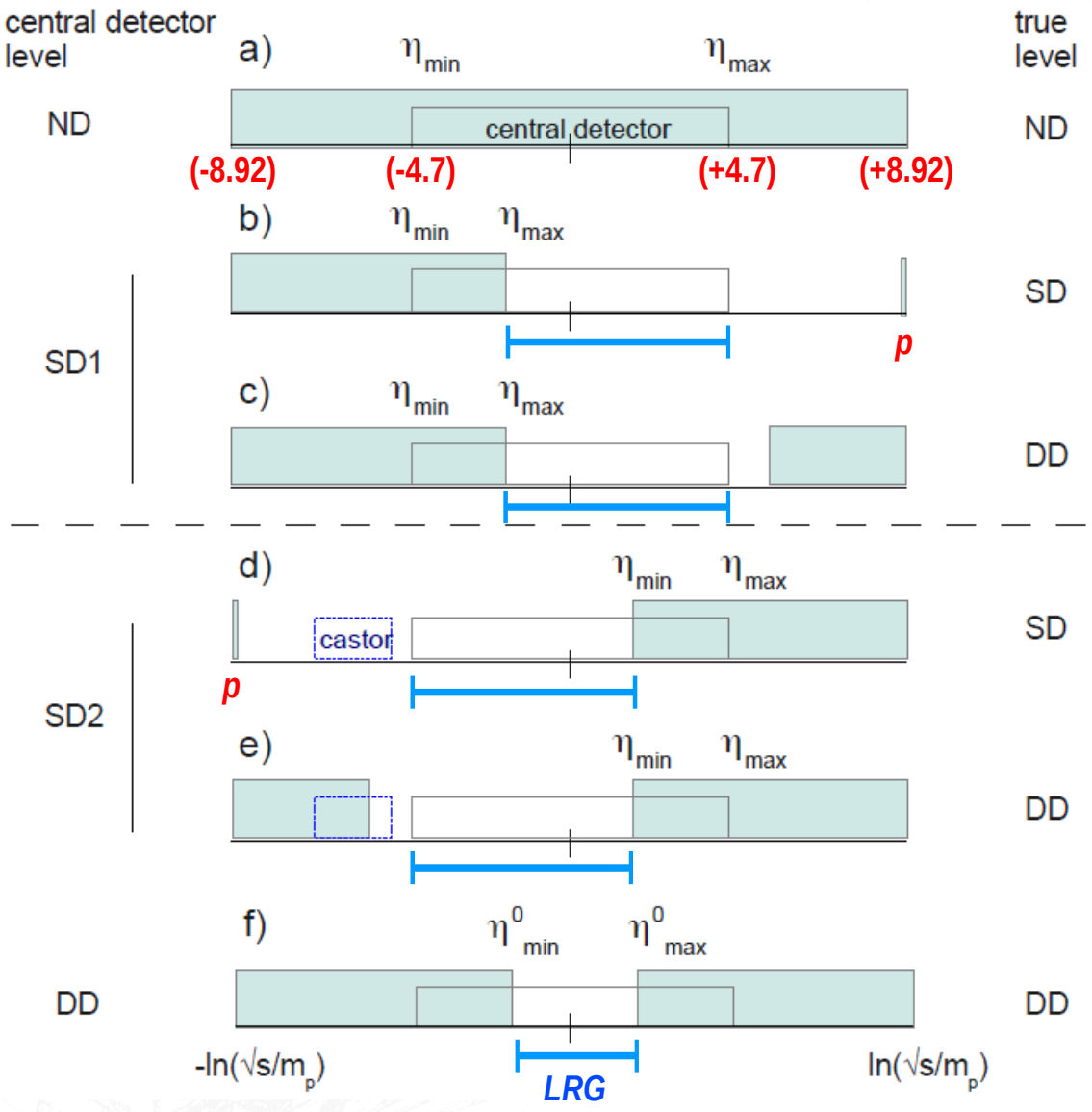

Detector-level distributions

- The gaps are defined as follows:
  - **Single dissociation**: $\Delta\eta^F \simeq 8.92 - \eta_{max}$ :: $\Delta\eta^F \simeq 8.92 + \eta_{min}$
  - **Double dissociation**: $\Delta\eta^0 = \eta^0_{max} - \eta^0_{min}$
- **Flattening** of the distribution is observed as an effect of diffractive events;

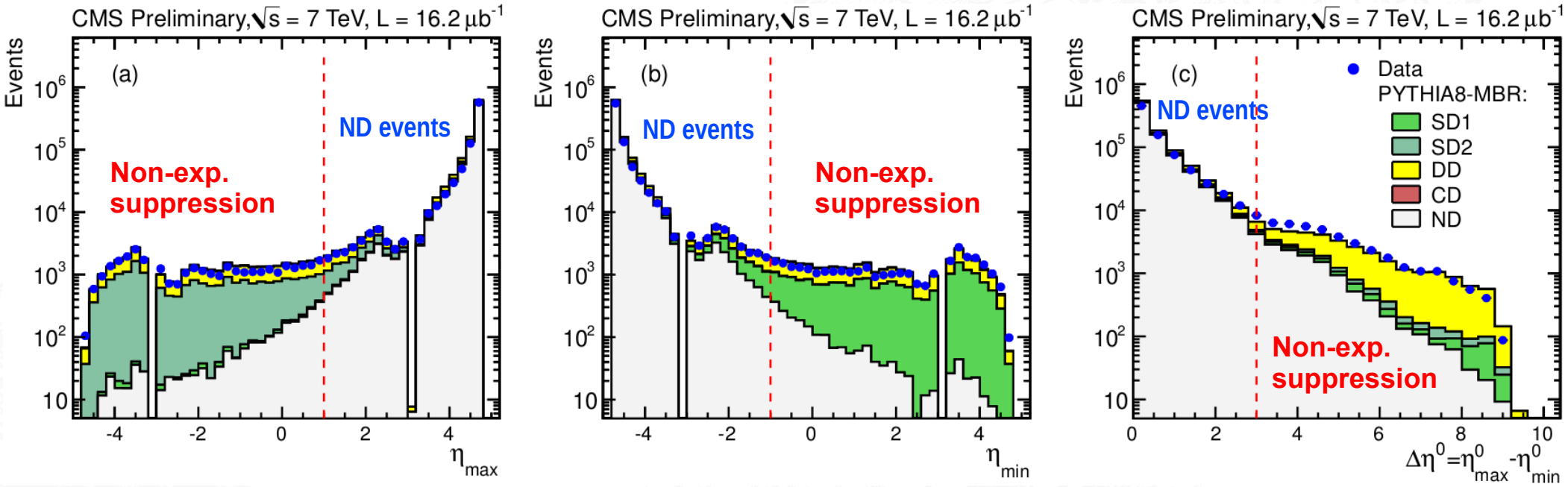

- Central LRG signature is imposed by the cuts: $\eta_{max} < 1$, $\eta_{min} > -1$ and $\Delta\eta^0 > 3$

Detector-level distributions

- DD events where one proton dissociates into a **low-mass systems** can escape the region of the central detector, or SD-like event;
- CASTOR is employed to select events with low-mass dissociated systems in the region of $-6.6 < \eta < -5.2$;

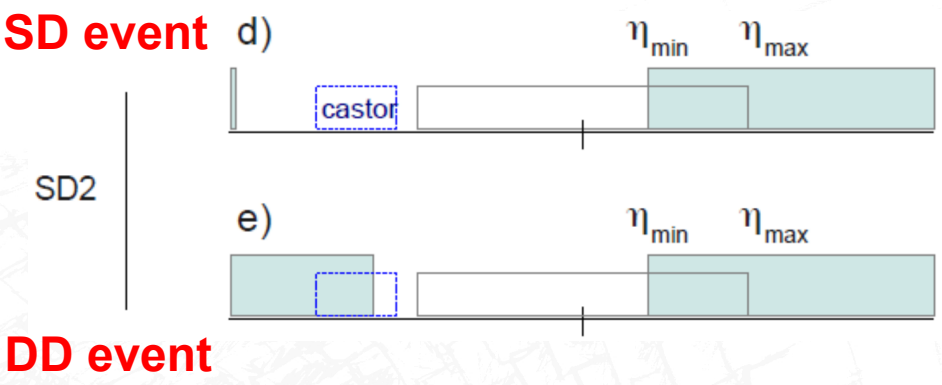

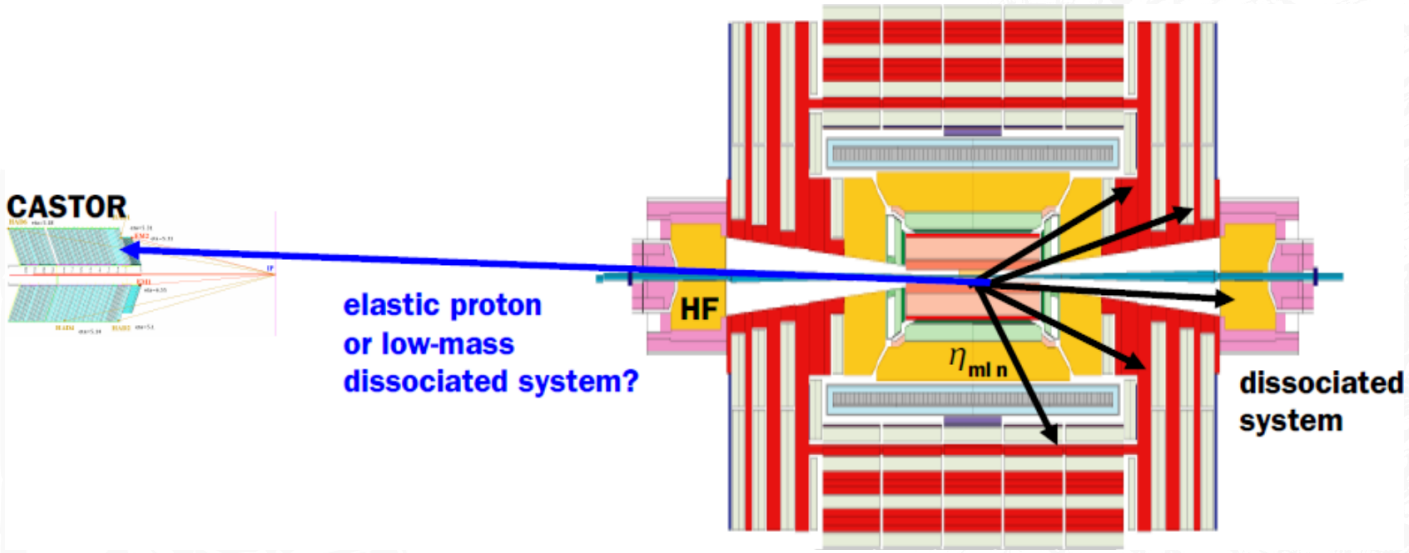

- **CASTOR tag**: selects events with signal above threshold of 1.48 GeV in at least one of the 16 sectors – summed over the first 5 modules;
- SD1-type events will be treated in a control sample, while **SD2-type events** will be used to estimate the diffraction cross secions.

Measurement

- The cross sections are measured based on the *fraction of longitudinal momentum loss of the incoming proton*:

$$\xi = \frac{M_X^2}{s} \qquad \Delta\eta^{SD} \simeq -log\xi$$

- The same is valid for DD events, altough M_X can be the **visible mass** of the dissociated system in the central detector;
- CASTOR has an acceptance of **$0.5 < \log_{10}(M_Y/GeV) < 1.1$** for the detection of the mass of the hadronic system outside the central detector;
- The variable ξ is determined at detector level in terms of the measured PF object:

$$\xi^{\pm} = \frac{\sum(E^i \mp p_z^i)}{\sqrt{s}}$$

  - E, p_z of the i^{th} PF object and both contributions in the ±z side.

- Due to events that **escape detection** in the central detector, the RECO ξ has to be corrected to match the true ξ: **$\log_{10} \xi_{corr} = \log_{10} \xi + C(\xi)$**

SD cross sections

- The differential cross sections are measured in bins of ξ:

$$\frac{d\sigma^{SD}}{d\log_{10}\xi} = \frac{N^{data}_{noCASTOR} - (N_{DD} + N_{CD} + N_{ND})^{MC}}{acc \cdot \mathcal{L} \cdot (\Delta \log_{10}\xi)_{bin}}$$

SD2

Background prediction

Acceptance + PU correction

Bin width

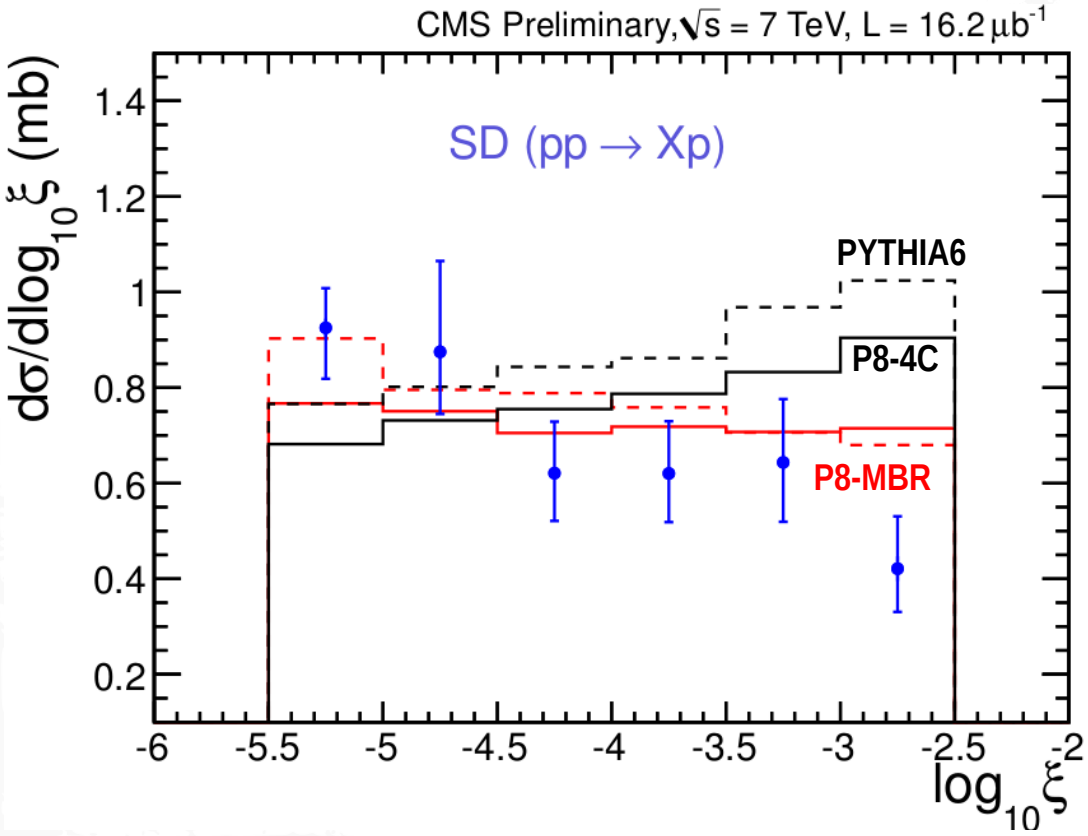

- **MBR** well describes the falling behavior of data;
- PYTHIA6 and 4C **fails**;

Total SD cross section at 7 TeV integrated over $-5.5 < \log_{10}\xi < -2.5$:

$4.27 \pm 0.004(\text{stat.})\ ^{+0.65}_{-0.58}\ (\text{syst.})$ mb

for both $pp \to Xp$ and $pp \to pY$ ($12 < M_X < 394$ GeV)

DD cross sections

- The differential cross sections for Double Diffraction are measured in both SD2+CASTOR and DD samples:

SD2

$$\frac{d\sigma^{DD}}{d\log_{10}\xi_X} = \frac{N^{data}_{CASTOR} - (N_{ND} + N_{SD} + N_{CD})^{MC}}{acc \cdot \mathcal{L} \cdot (\Delta \log_{10}\xi_X)_{bin}}$$

DD

$$\frac{d\sigma^{DD}}{d\Delta\eta} = \frac{N^{data} - (N_{ND} + N_{SD} + N_{CD})^{MC}}{acc \cdot \mathcal{L} \cdot (\Delta\eta)_{bin}}$$

Acceptance + PU correction

bin width

Total DD cross section at 7 TeV integrated over $\Delta\eta > 3$ and $M_{X,Y} > 10$ GeV:

$0.93 \pm 0.01(\text{stat.})\ ^{+0.26}_{-0.22}\ (\text{syst.})$ mb

Error bars: dominated by systematic uncertainties

Trajectory with ε = 0.08 is favored in DD events

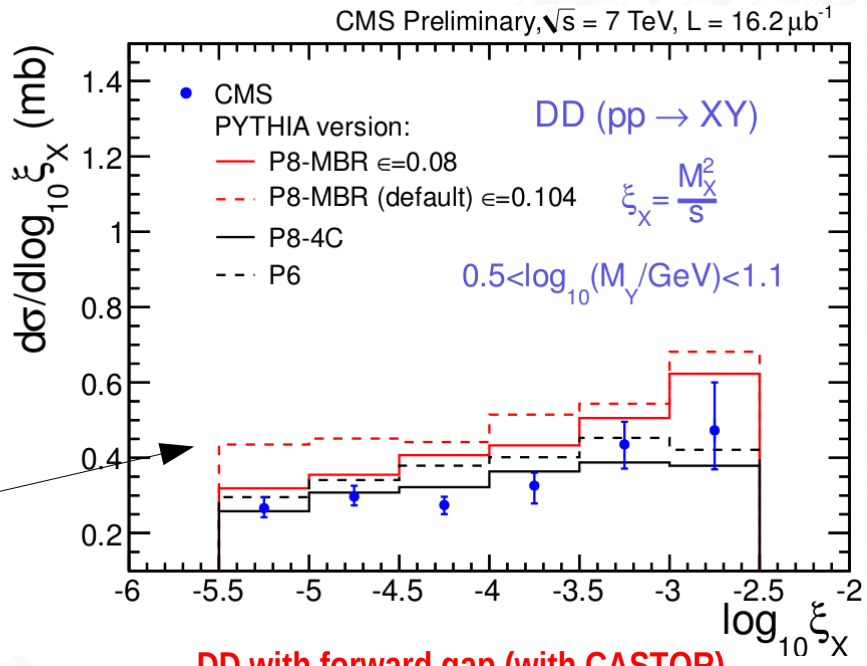

DD with forward gap (with CASTOR)

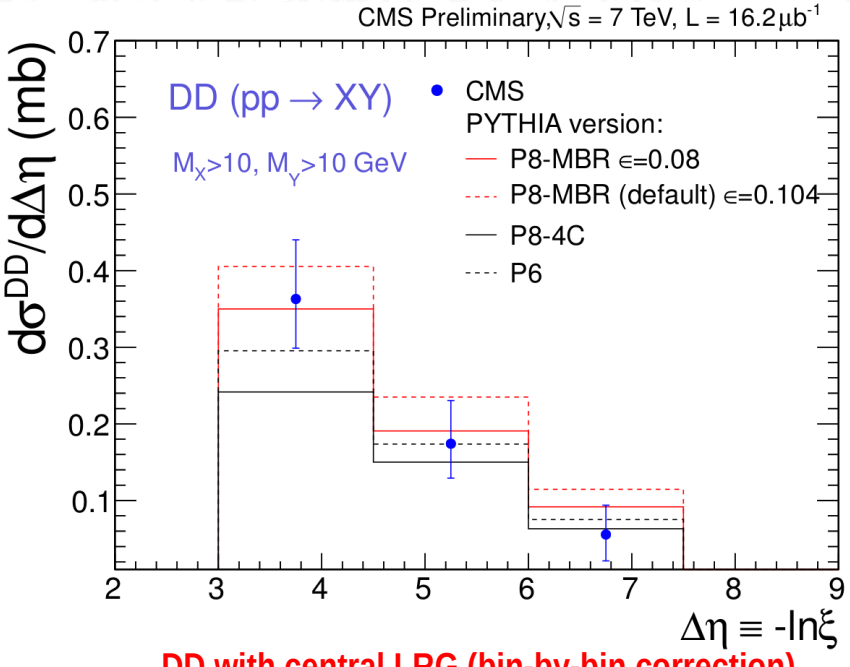

DD with central LRG (bin-by-bin correction)

Rapidity gap cross section

- The measurement of the forward rapidity gap in terms of the **largest forward rapidity gap** $\Delta\eta^F$;
- Data has to be **corrected** for background of circulating beams and for bin migration and fake/miss events with the Bayesian unfolding method;
- Unfolded and fully corrected differential cross section of the forward rapidity gap size:

p_T > 200 MeV, |η|<4.7

Total systematic uncertainty ≲20%

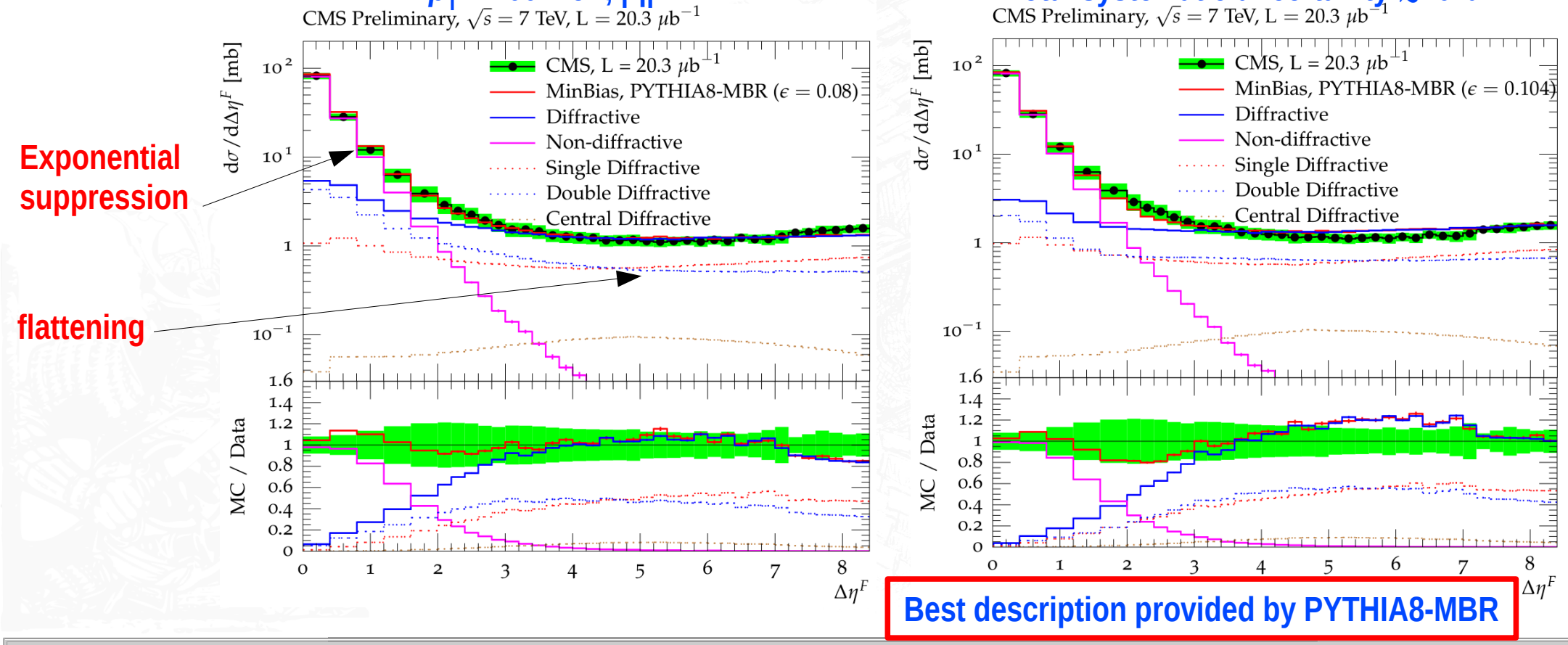

Best description provided by PYTHIA8-MBR

Comparison to ATLAS results

- Hadron level definition in each measurement: CMS: |η|<4.7, ATLAS: |η|<4.9.

- The CMS results present a good agreement wih ATLAS measuarement within the uncertainties;

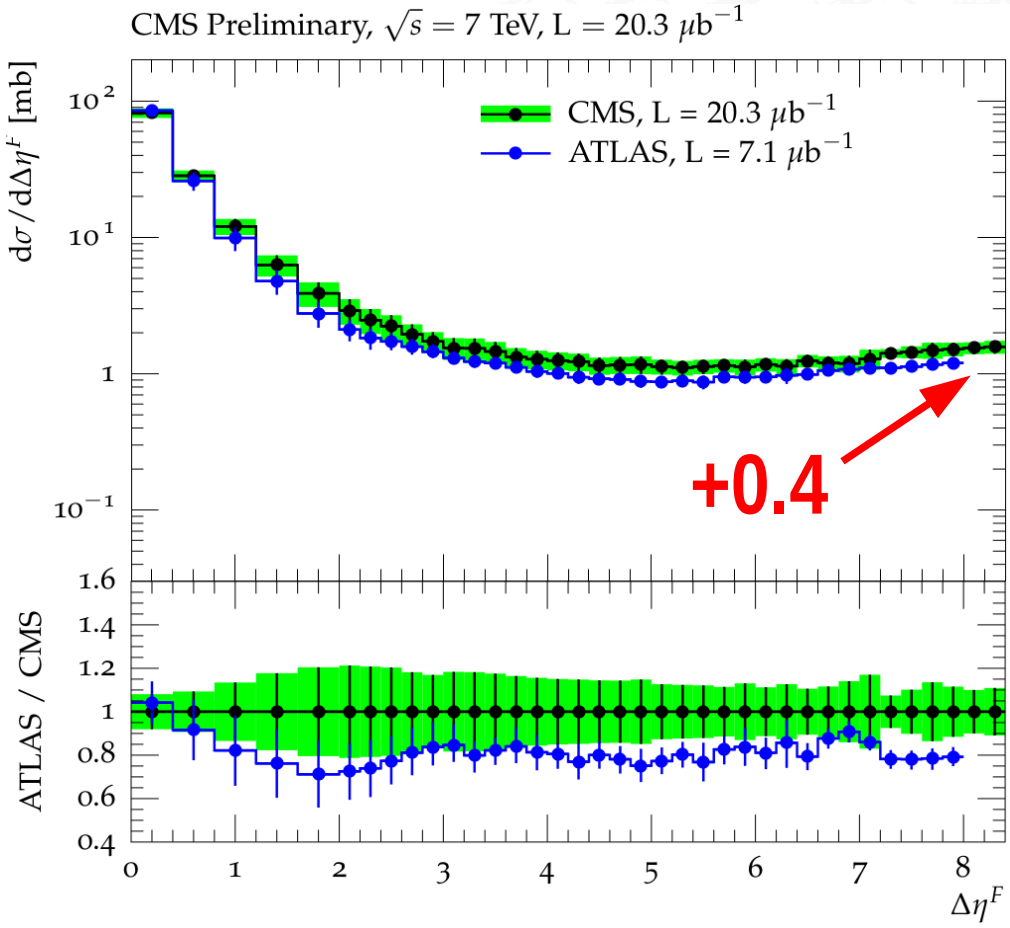

Outline

- CMS detector and capabilities for forward physics;
- Diffractive & Exclusive processes in CMS;
- Measurement of diffractive dissociation cross sections in CMS;
  - Single diffraction (forward gap + no CASTOR);
  - Double diffraction (forward gap + CASTOR) – low & high masses;
  - Double diffraction (central gap) – high masses.

- Exclusive production of massive electroweak-boson pairs;
  - Measurement of exclusive $\gamma\gamma \to \mu^+\mu^-$ at large masses – control;
  - Search for exclusive $\gamma\gamma \to W^+W^-$ production;
  - Limits on anomalous quartic gauge couplings.

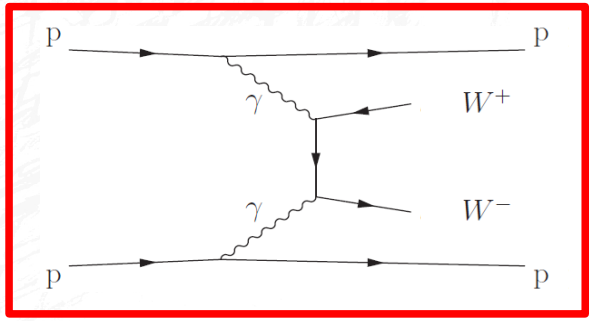

JHEP 07 (2013) 116

Event selection for leptons

- Data collected in 2011 by the CMS detector at 7 TeV:
  - Final state: $W^+W^- \to e^\pm\mu^\mp\nu\nu$ to suppress DY bkg;
  - Events with opposite-sign and flavor leptons: **5.05 fb^{-1}**;
  - Events with opposite-sign muon: **5.24 fb^{-1}** (control sample).
- Leptons are selected with the requirements:
  - $p_T(\ell) > 20$ GeV and $|\eta(\ell)| < 2.4$;
  - $m(\ell^+\ell^-) > 20$ GeV and $p_T(\ell^+\ell^-) > 30$ GeV.
- Events are selected vertices consistent with two lepton tracks and **nothing else**;
- **aQGC**: search is performed in the kinematical region with $p_T(\mu e) > 100$ GeV.

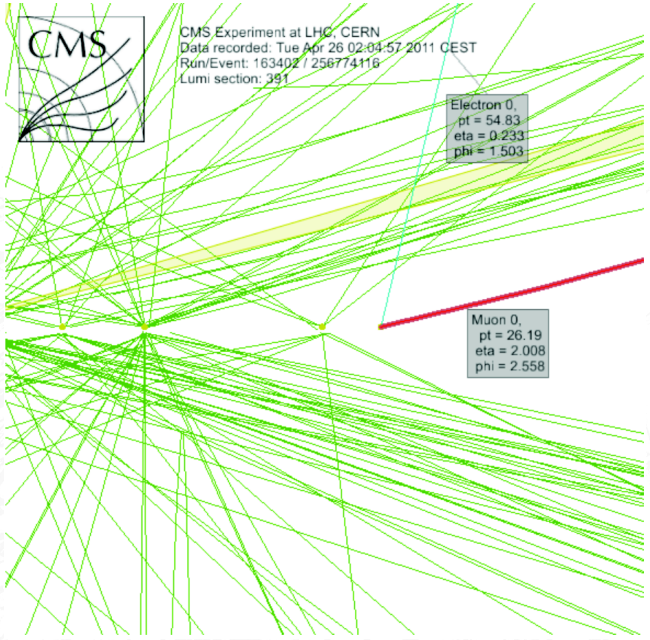

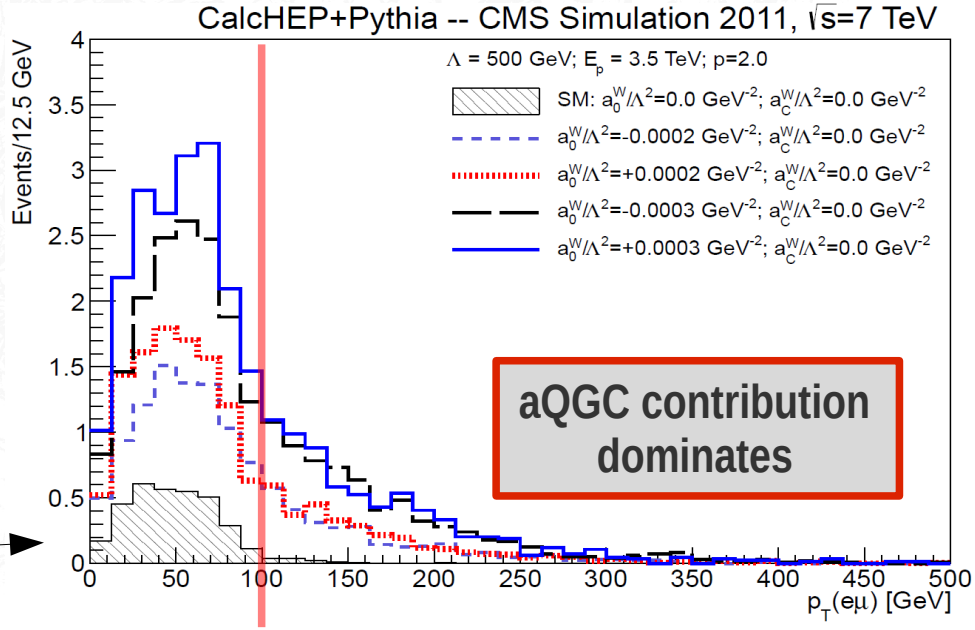

Measurement of $\gamma\gamma \rightarrow \mu^+\mu^-$

- The study is performed in **two different kinematic regions** in order to discriminate the dominant contributions of elastic and inelastic interactions;
- **Elastic region** is defined by the exclusivity selection by applying the following kinematical cuts:
  - $p_T(\ell)$ balance below 1 GeV;
  - Back-to-back leptons with $\Delta\varphi > 0.9\pi$.
- The regions are defined as follows:

Good agreement with LPAIR

Elastic	Inelastic (quasi-exclusive)
$1-\lvert\Delta\varphi(\ell^+\ell^-)/\pi\rvert < 0.1$ $\lvert\Delta p_T(\ell^+\ell^-)\rvert < 1.0$	$1-\lvert\Delta\varphi(\ell^+\ell^-)/\pi\rvert > 0.1$ $\lvert\Delta p_T(\ell^+\ell^-)\rvert > 1.0$

Dissociation dominates

ELASTIC REGION

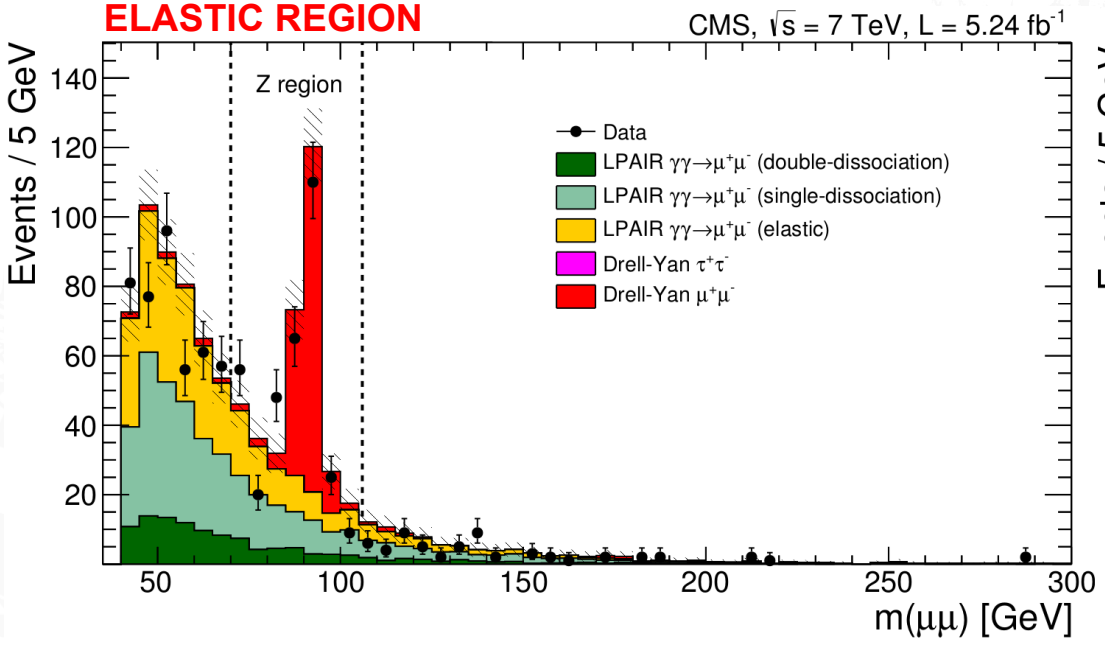

INELASTIC REGION

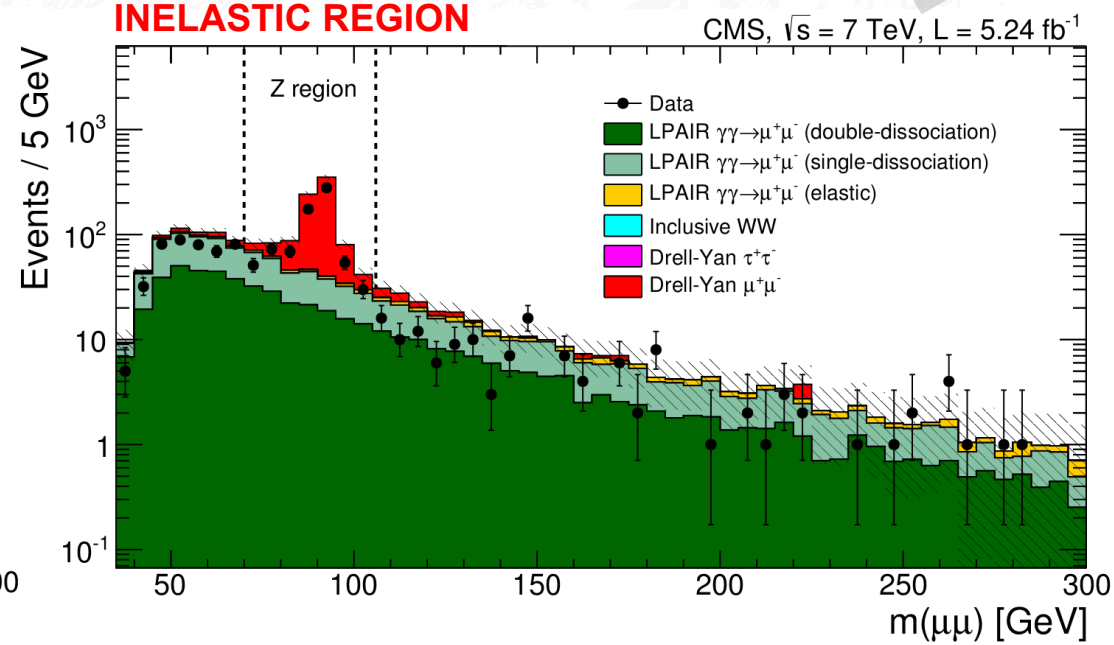

Proton dissociation in inelastic $\gamma\gamma \rightarrow \mu^+\mu^-$

- A deficit is observed in data which is **not** predicted by LPAIR – **rescattering effects** not included to the predictions;

Region	Data	Simulation	Data/Simulation
Elastic	820	906 ± 9	0.91 ± 0.03
Dissociation	1312	1830 ± 17	0.72 ± 0.02
Total	2132	2736 ± 19	0.78 ± 0.02

- Proton dissociation in LPAIR is **loosely** constrained experimentally – a normalization factor can be employed for this component;

- We estimate a normalization factor for masses larger than the WW mass:

$$F = \left. \frac{N_{\mu\mu\ data} - N_{DY}}{N_{elastic}} \right|_{m(\mu^+\mu^-)>160\ \mathrm{GeV}}$$

$$= \boxed{3.23 \pm 0.53.}$$

- This factor is then used to re-scale the signal cross section in order to include the contribution from the **proton dissociation**.

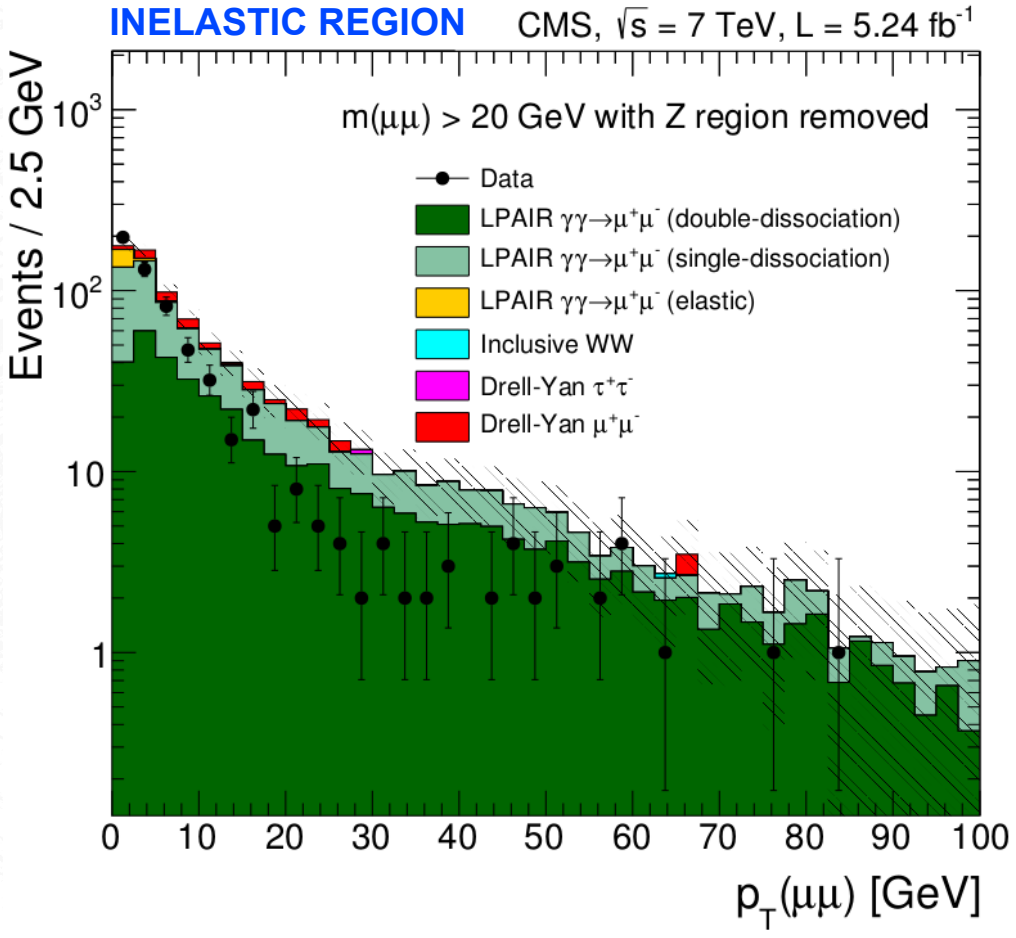

Exclusive $\gamma\gamma \to W^+W^-$: theory

- The $\gamma\gamma \to W^+W^-$ coupling is present in the SM Lagrangian: quartic coupling plus t- and u-channel W exchange;

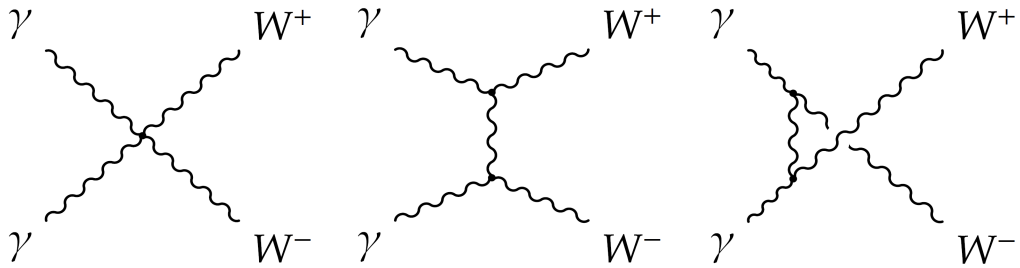

- Extension to consider the **anomalous quartic gauge couplings** (aQGC):

$$L_6^0 = \frac{-e^2}{8}\frac{a_0^W}{\Lambda^2}F_{\mu\nu}F^{\mu\nu}W^{+\alpha}W^-_\alpha - \frac{e^2}{16\cos^2\Theta_W}\frac{a_0^Z}{\Lambda^2}F_{\mu\nu}F^{\mu\nu}Z^\alpha Z_\alpha,$$

$$L_6^C = \frac{-e^2}{16}\frac{a_C^W}{\Lambda^2}F_{\mu\alpha}F^{\mu\beta}(W^{+\alpha}W^-_\beta - W^{-\alpha}W^+_\beta) - \frac{e^2}{16\cos^2\Theta_W}\frac{a_C^Z}{\Lambda^2}F_{\mu\alpha}F^{\mu\beta}Z^\alpha Z_\beta,$$

AQGC† parameters

Λ: scale for New Physics

- Form factors are included in order to tame the rising of the cross section:

$$a_{0,C}^W(W_{\gamma\gamma}^2) = \frac{a_{0,C}^W}{\left(1+\frac{W_{\gamma\gamma}^2}{\Lambda^2}\right)^p}$$

$W_{\gamma\gamma}$: **$\gamma\gamma$ c.m. energy**

p **= 2**
(dipole form factor)

- For a_0^W/Λ^2, $a_C^W/\Lambda^2 \sim 10^{-5}$: unitairy bound reached, so **Λ = 500 GeV**.

† Belanger, G.; Boudjema, F.; Phys. Lett. B 288 (1992) 201

Signal from $W^+W^- \to \mu^\pm e^\mp \nu\bar{\nu}$

- Events passing all the requirements:

Signal: **2.2 ± 0.4 evt**
Bkg: **0.84 ± 0.15 evt**

Selection step	Signal $\epsilon \times A$	Events in data
Trigger and preselection	28.5%	9086
$m(\mu^\pm e^\mp) > 20$ GeV	28.0%	8200
Muon ID and Electron ID	22.6%	1222
$\mu^\pm e^\mp$ vertex with 0 extra tracks	13.7%	6
$p_T(\mu^\pm e^\mp) > 30$ GeV	10.6%	2

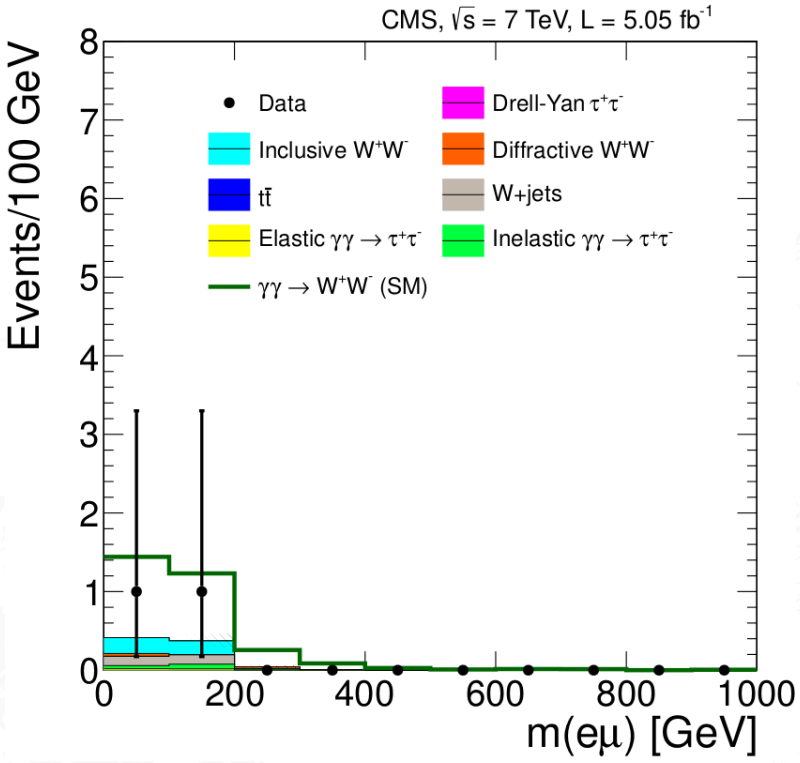

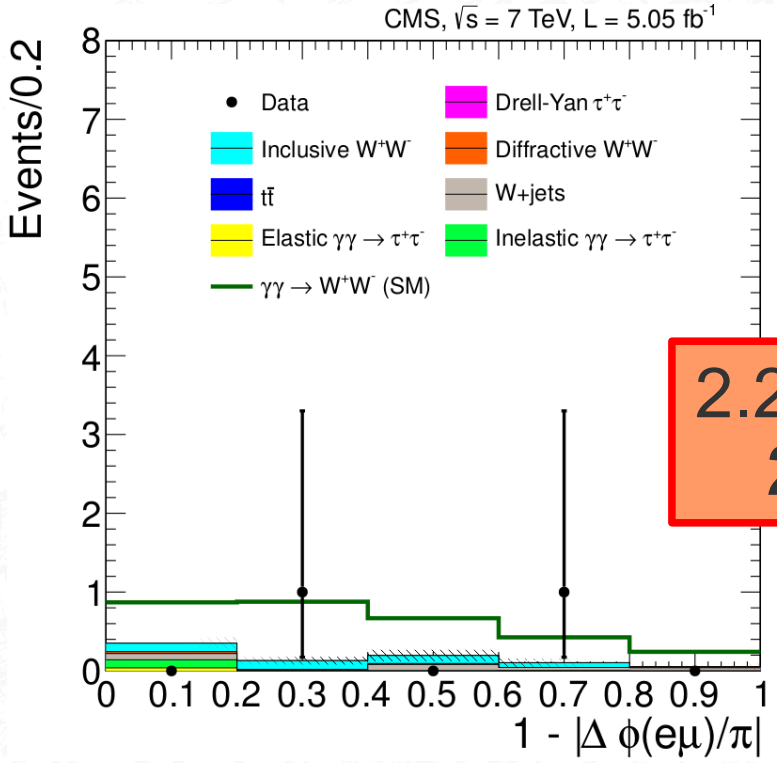

2.2 evt expected
2 observed

SM: 4.0 ± 0.7 fb

σ · BR with 95% CL: $\sigma(pp \to p^{(*)}W^+W^-p^{(*)} \to p^{(*)}\mu^\pm e^\mp p^{(*)}) = 2.1^{+3.1}_{-1.9}$ fb

Search for aQGC

- The upper limit on the cross section times Branching fraction is found as

$$\sigma(pp \to p^{(*)}W^+W^-p^{(*)} \to p^{(*)}\mu^{\pm}e^{\mp}p^{(*)}) < 10.6\,\text{fb}$$

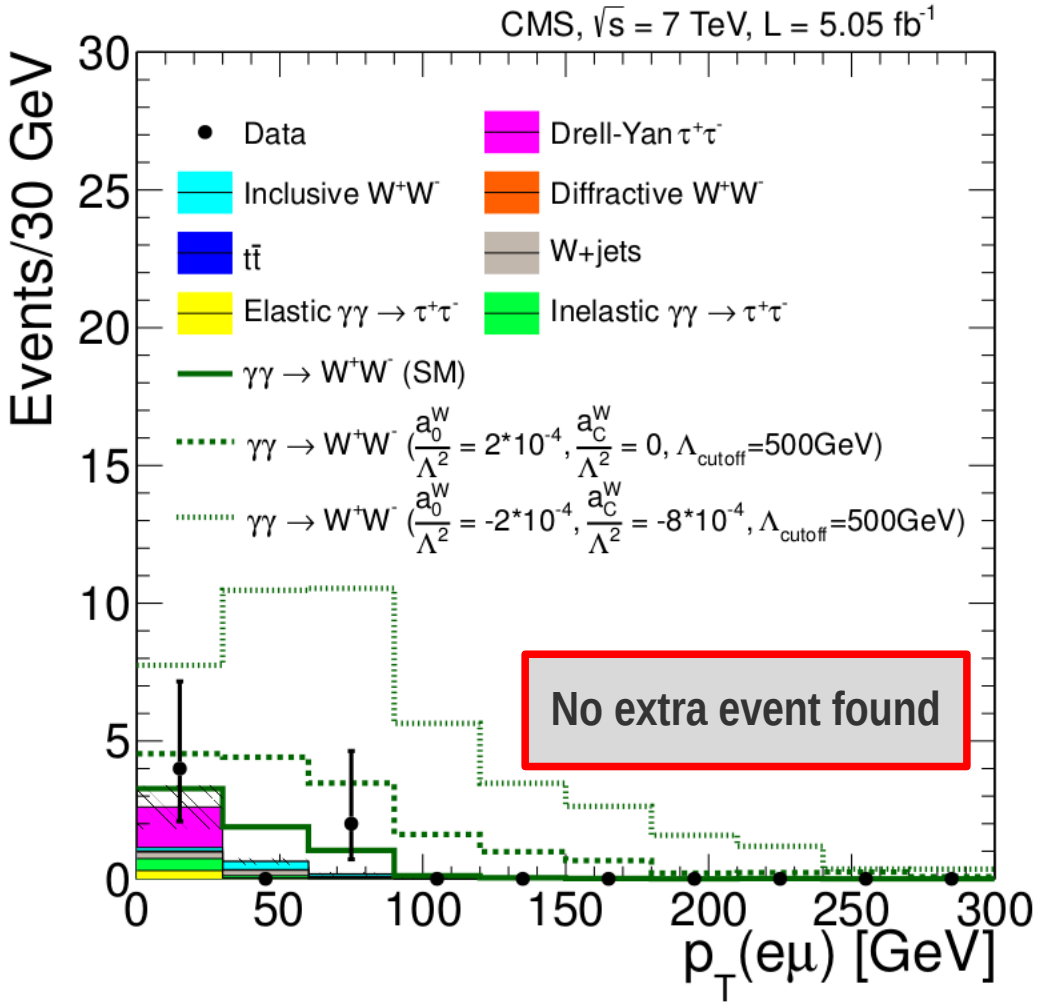

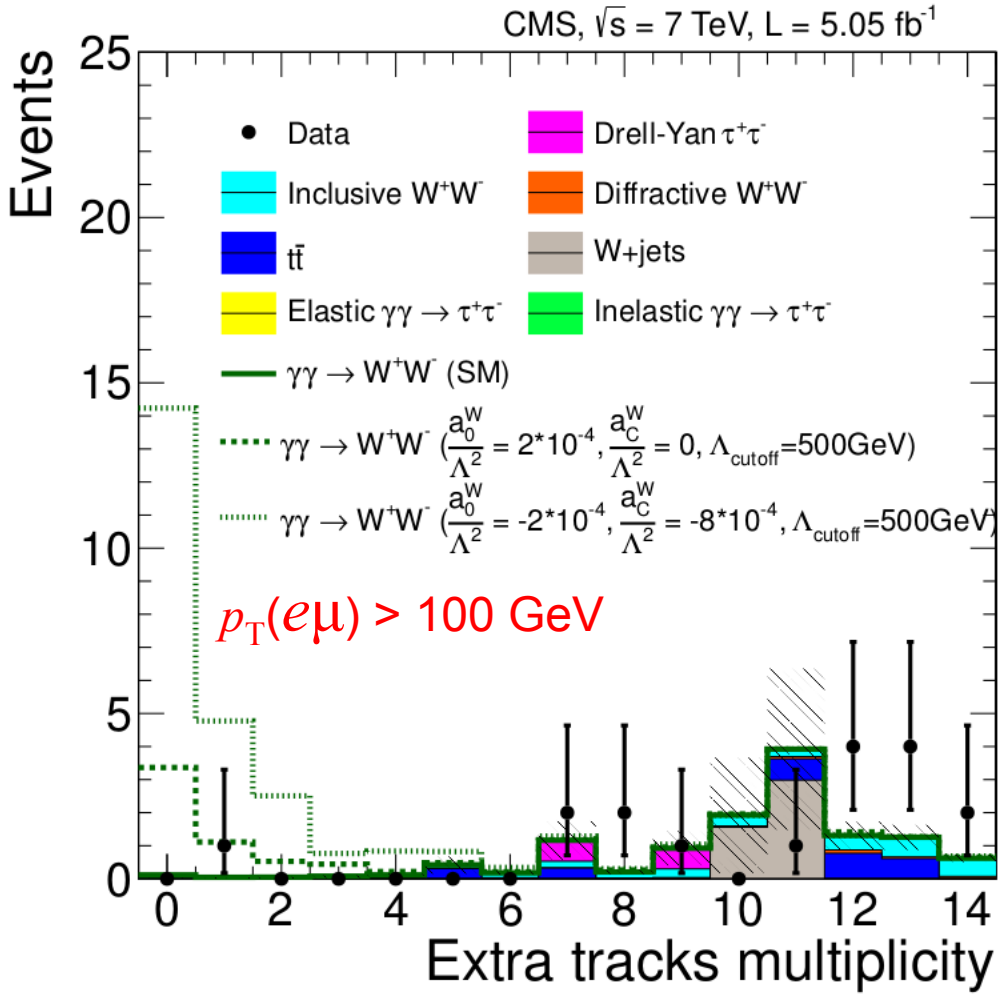

Limits on aQGC

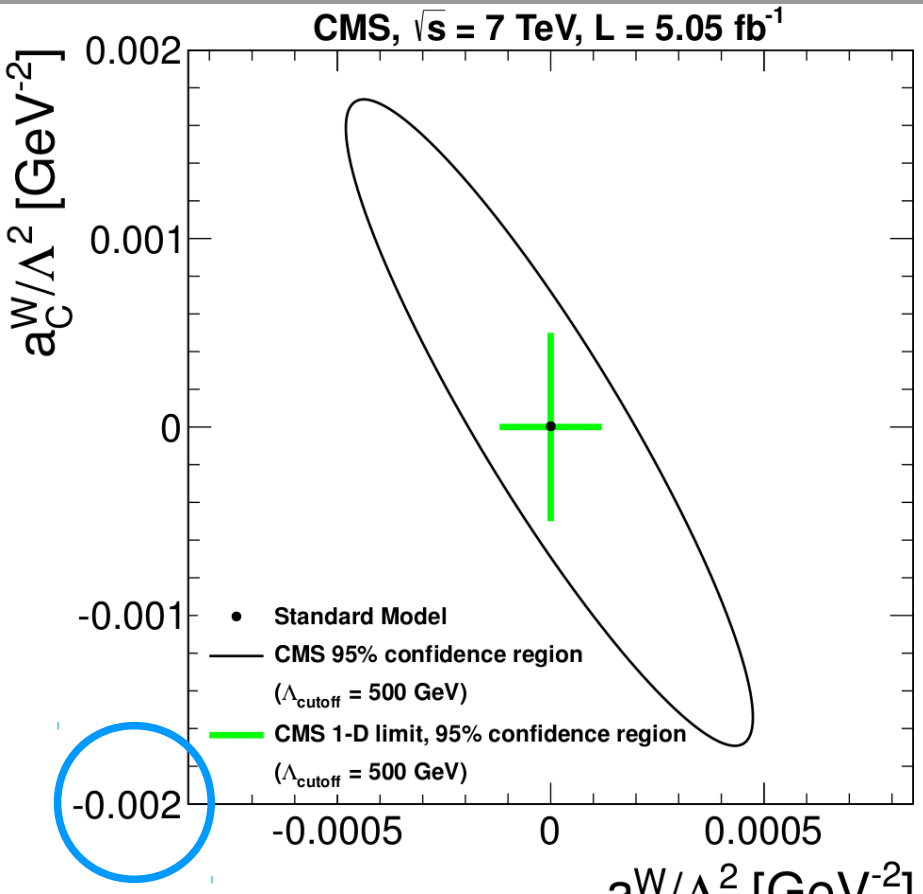

OPAL

Scales differ by a factor of **10** and **100**

DØ

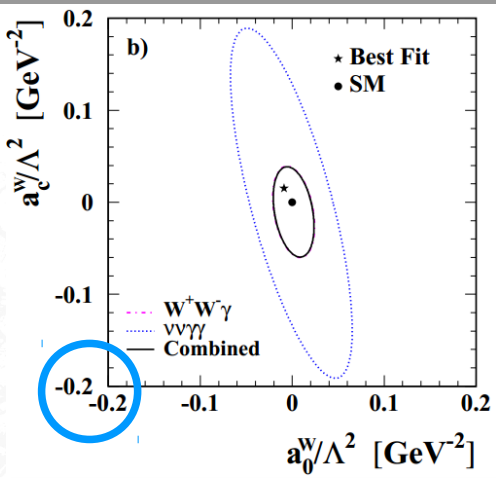

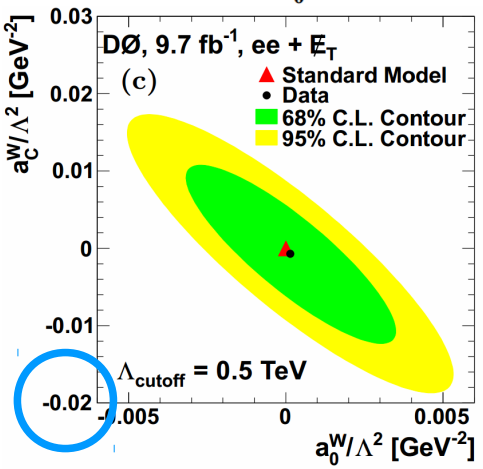

- The upper limit on the cross section-times-branching fraction is found as

$$-0.00015 < a_0^{\mathrm{W}}/\Lambda^2 < 0.00015\,\mathrm{GeV}^{-2}\ (a_C^{\mathrm{W}}/\Lambda^2 = 0, \Lambda_{\mathrm{cutoff}} = 500\,\mathrm{GeV}),$$
$$-0.0005 < a_C^{\mathrm{W}}/\Lambda^2 < 0.0005\,\mathrm{GeV}^{-2}\ (a_0^{\mathrm{W}}/\Lambda^2 = 0, \Lambda_{\mathrm{cutoff}} = 500\,\mathrm{GeV}).$$

$$-4.0 \times 10^{-6} < a_0^{\mathrm{W}}/\Lambda^2 < 4.0 \times 10^{-6}\,\mathrm{GeV}^{-2}\ (a_C^{\mathrm{W}}/\Lambda^2 = 0, \text{no form factor}),$$
$$-1.5 \times 10^{-5} < a_C^{\mathrm{W}}/\Lambda^2 < 1.5 \times 10^{-5}\,\mathrm{GeV}^{-2}\ (a_0^{\mathrm{W}}/\Lambda^2 = 0, \text{no form factor}).$$

Limits 2 orders of magn. more stringent than those from LEP

Summary

- CMS has successifully measured exclusive processes at **high masses** and **diffractive events**;
- Diffraction cross sections have been measured in CMS:
  - **Single Diffraction** ($-5.5 < \log_{10}\xi < -2.5$): $\mathbf{4.27 \pm 0.004(stat.)\,^{+0.65}_{-0.58}\ (syst.)\ mb}$
  - **Double Diffraction** ($\Delta\eta > 3$, $M_{X,Y} > 10$ GeV): $\mathbf{0.93 \pm 0.01(stat.)\,^{+0.26}_{-0.22}\ (syst.)\ mb}$

  with results extending previous measurements of ATLAS;
- The search for the exclusive production of W pairs results in **two potential candidates** with observed cross section in agreement with the SM expectation:

$$\sigma(\mathrm{pp} \to \mathrm{p}^{(*)}\mathrm{W}^{+}\mathrm{W}^{-}\mathrm{p}^{(*)} \to \mathrm{p}^{(*)}\mu^{\pm}\mathrm{e}^{\mp}\mathrm{p}^{(*)}) = 2.2^{+3.3}_{-2.0}\,\mathrm{fb},$$

- aQGC limits:

$$-0.00015 < a_0^{\mathrm{W}}/\Lambda^2 < 0.00015\,\mathrm{GeV}^{-2}\ (a_C^{\mathrm{W}}/\Lambda^2 = 0, \Lambda_{\mathrm{cutoff}} = 500\,\mathrm{GeV}),$$
$$-0.0005 < a_C^{\mathrm{W}}/\Lambda^2 < 0.0005\,\mathrm{GeV}^{-2}\ (a_0^{\mathrm{W}}/\Lambda^2 = 0, \Lambda_{\mathrm{cutoff}} = 500\,\mathrm{GeV}).$$

  - **Two orders of magnitude** more stringent than those determined by the LEP and Tevatron results.

Backup slides

The CMS experiment

CASTOR: 5.3 < |η| < 6.6
ZDC: |η| > 8.1
(**not used in these analyses**)

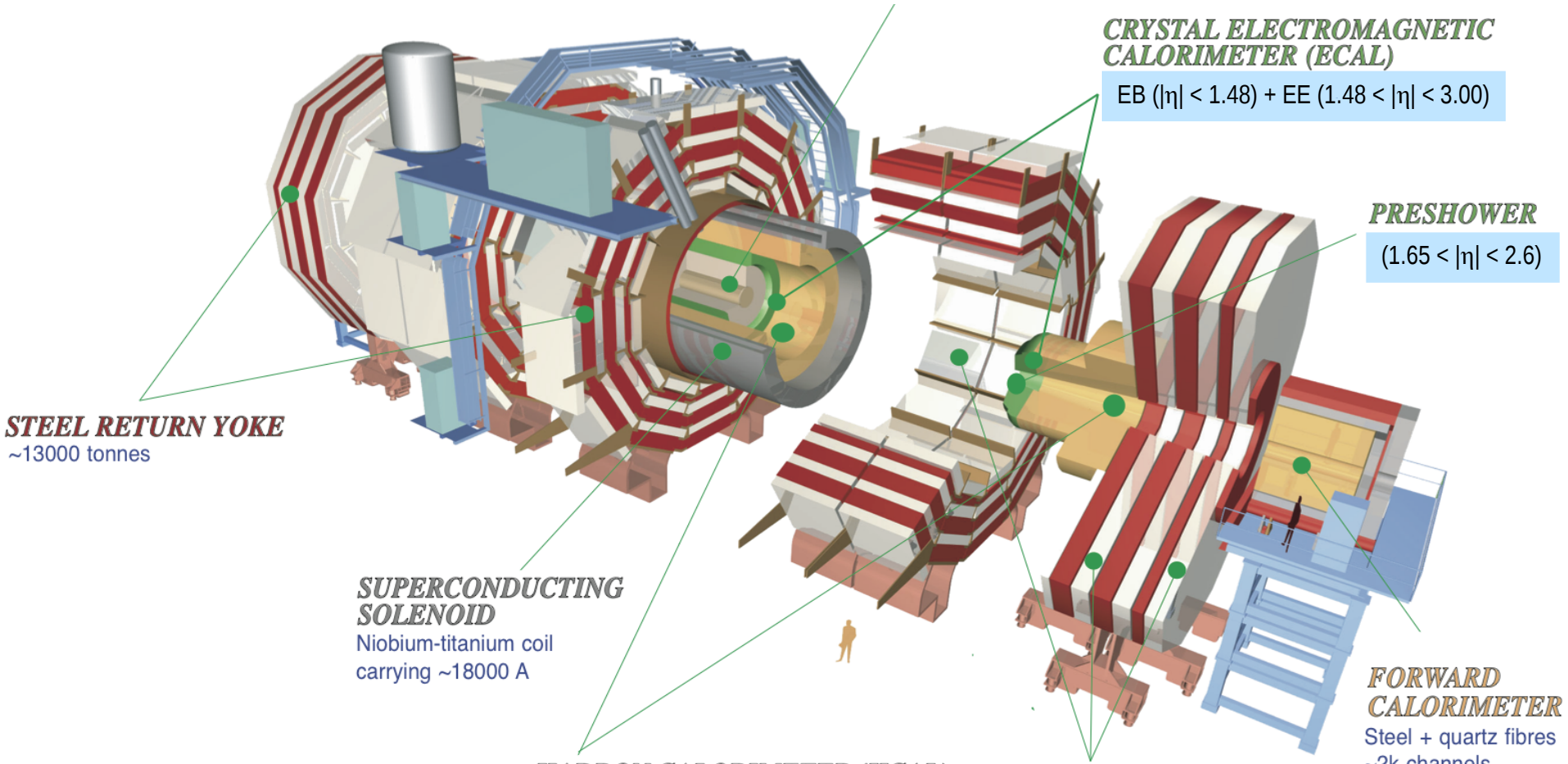

Total weight : 14000 tonnes
Overall diameter : 15.0 m
Overall length : 28.7 m
Magnetic field : 3.8 T

Correction factor for RECO ξ

- The reconstructed ξ has to be corrected due to the events that **escape detection** in the central detector and particles below the PF object threshold:

$$\xi^{\pm} = \frac{\sum(E^i \mp p_z^i)}{\sqrt{s}} \longrightarrow C(\xi) \longrightarrow \xi = \frac{M_X^2}{s}$$

- The correction factor C(ξ) is defined as: $\log_{10}\xi_{corr} = \log_{10}\xi + C(\xi)$

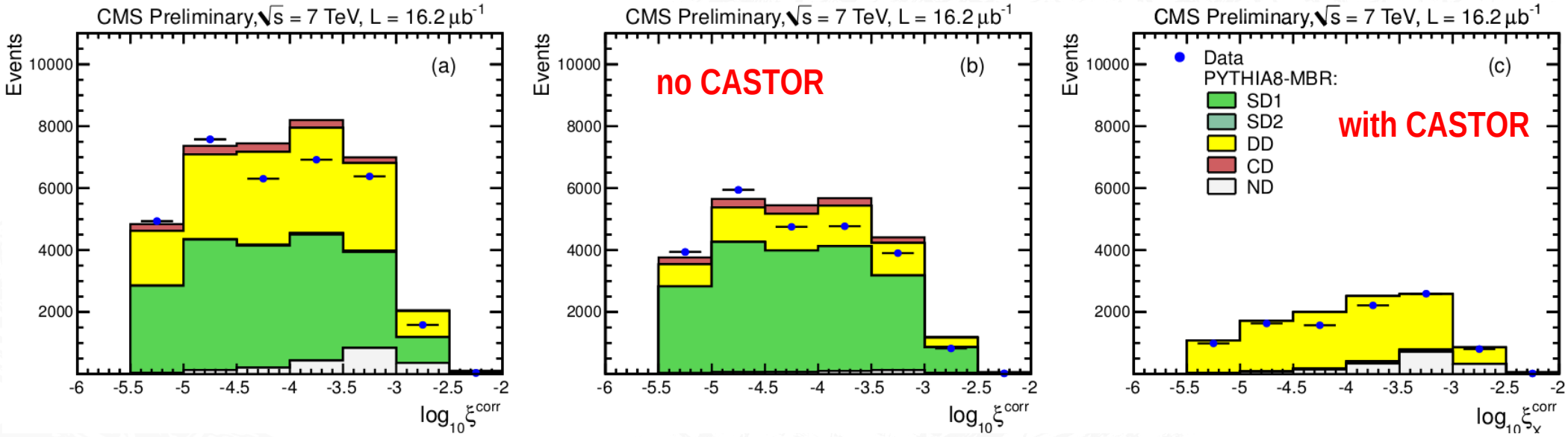

- **PYTHIA8-MBR** (with renormalized flux) shows better results than PYTHIA8-4C.

Elastic region for $\gamma\gamma \rightarrow \mu^+\mu^-$

- Although a good agreement with the MC predictions in the elastic region, the background from muon pairs produced via Drell-Yan is significative;
  - The mass region of Z-boson resonance is investigated.

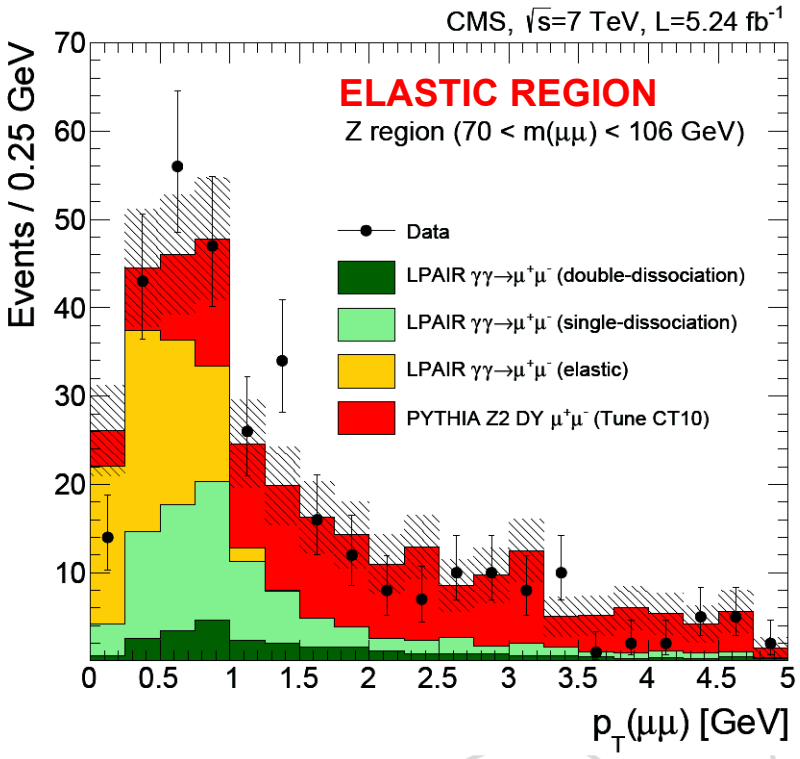

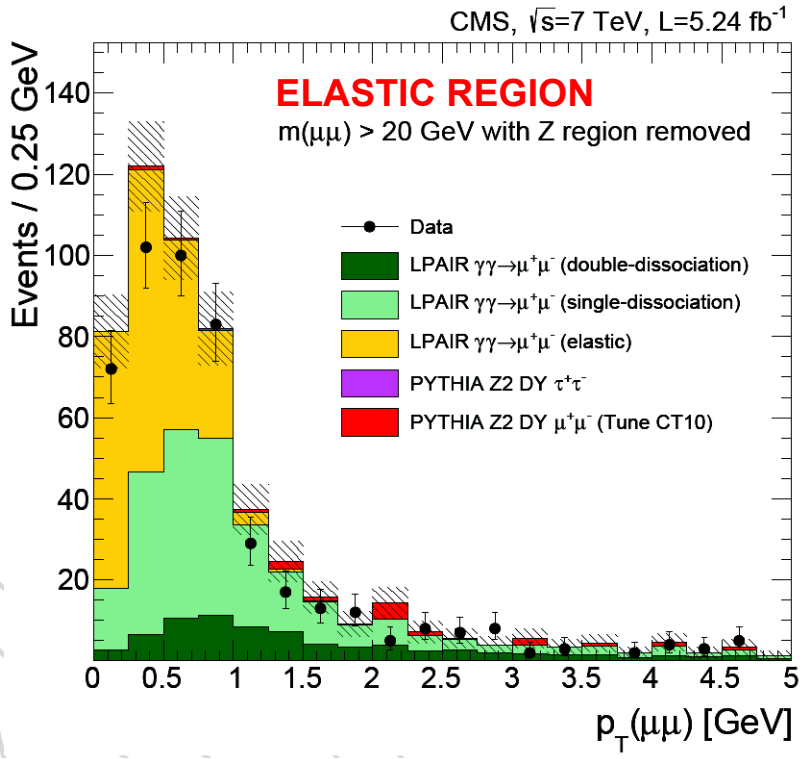

- The contribution from both regions can be accounted in Data and MC:

Region	Data	Simulation	Data/Simulation
Elastic	820	906 ± 9	0.91 ± 0.03
Dissociation	1312	1830 ± 17	0.72 ± 0.02
Total	2132	2736 ± 19	0.78 ± 0.02

Invariant mass for $\gamma\gamma \to \mu^+\mu^-$

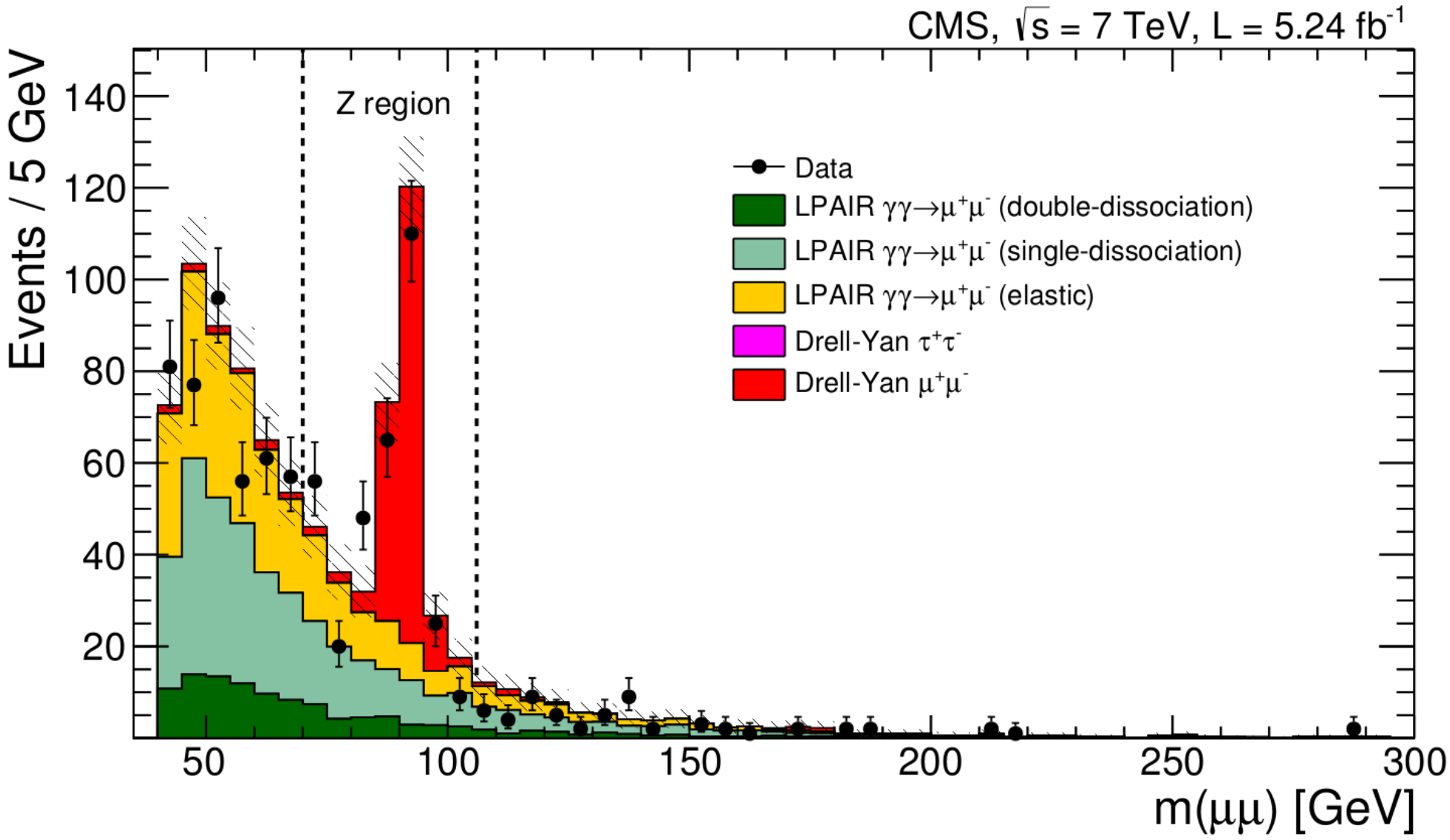

Acoplanarity for $\gamma\gamma \to \mu^+\mu^-$

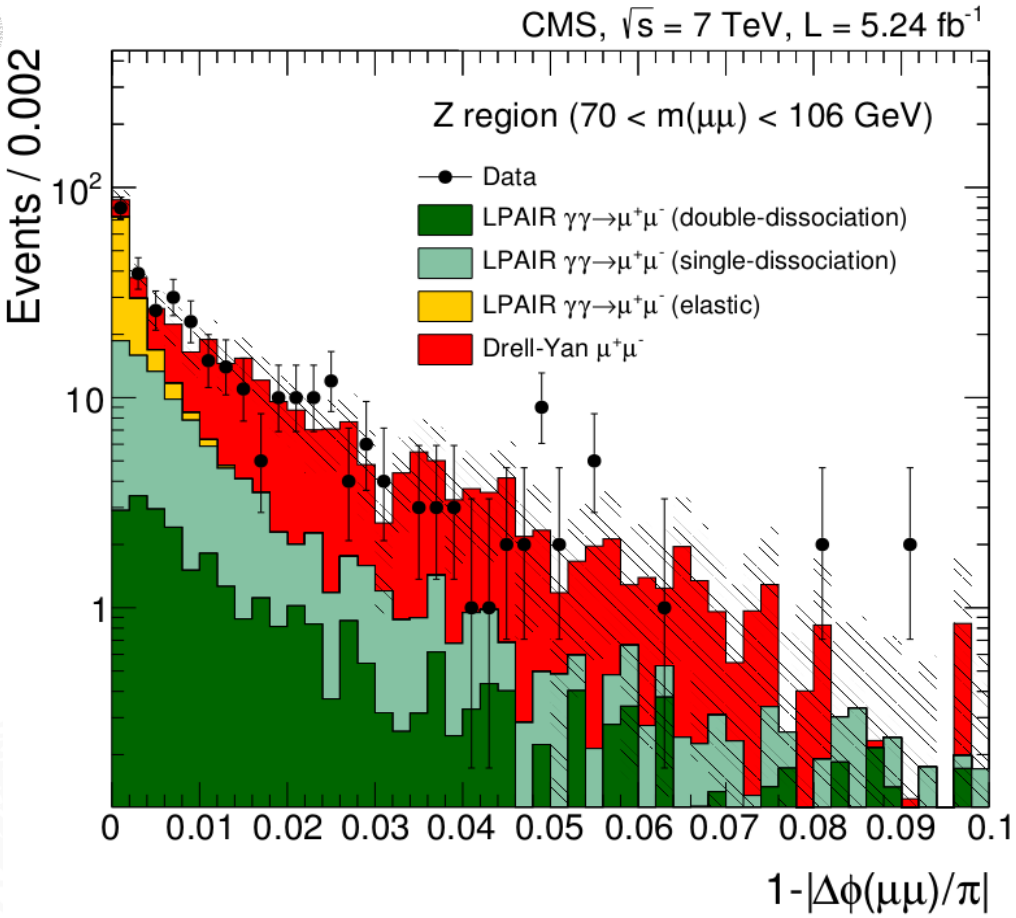

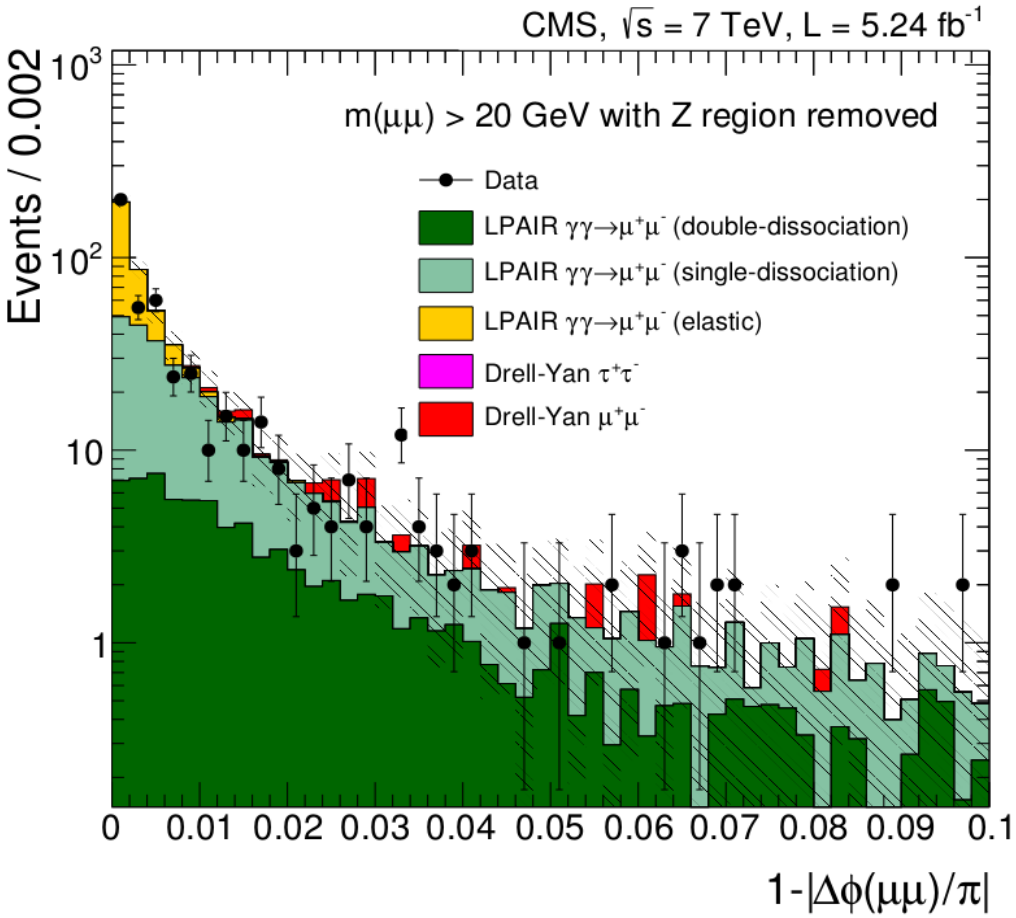

Transverse momentum for $\gamma\gamma \to \mu^+\mu^-$

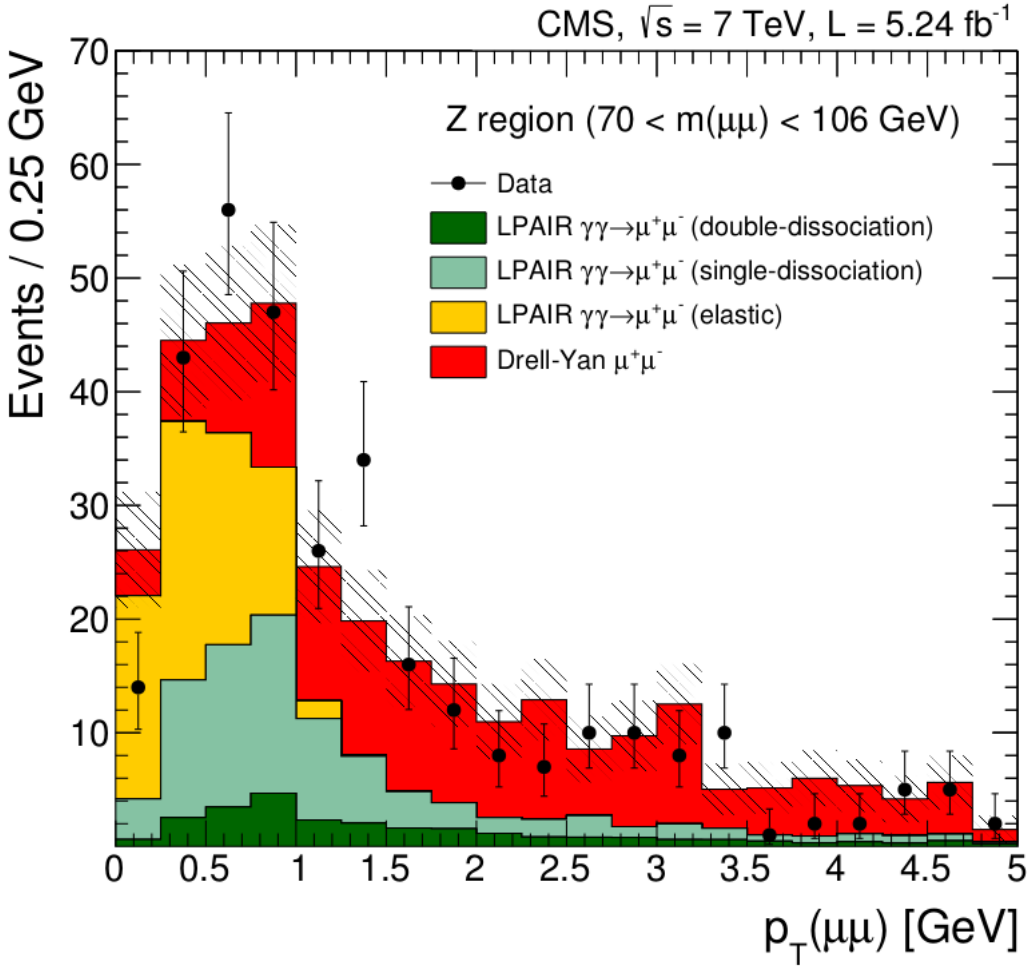

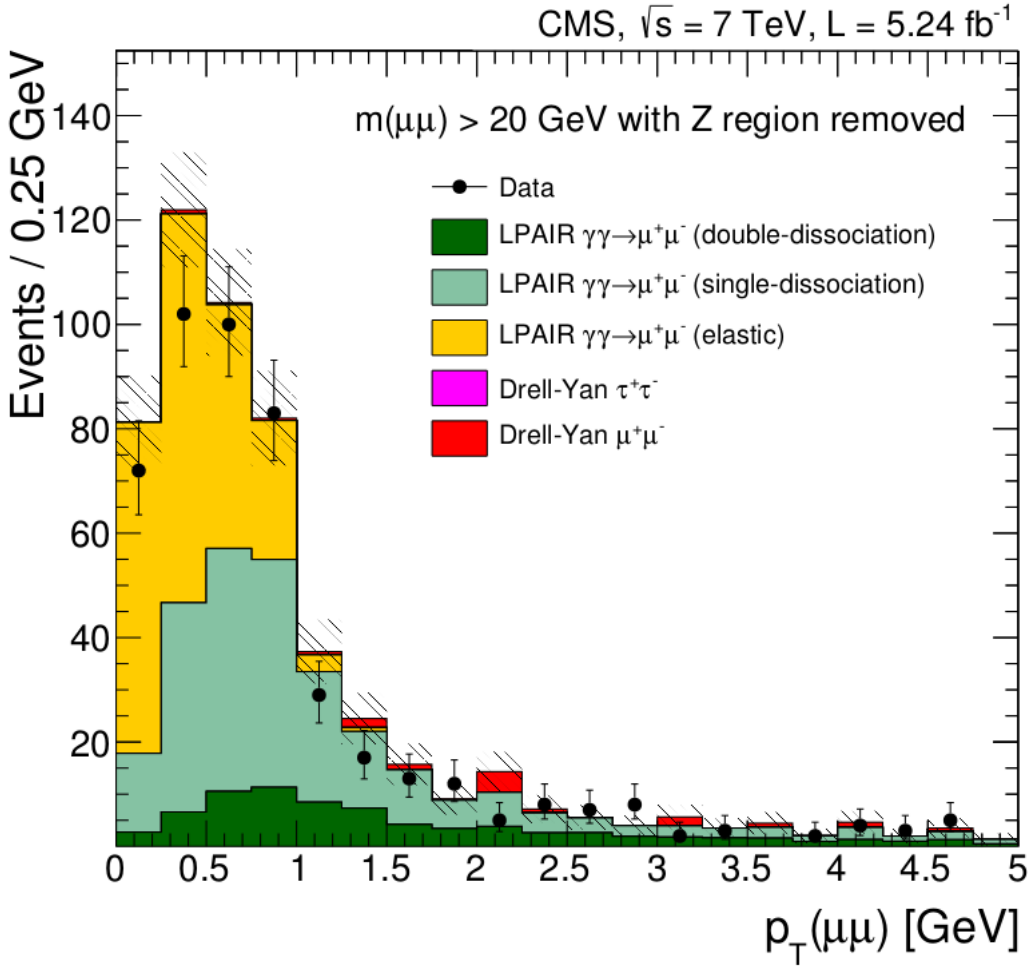

Transverse momentum for $\gamma\gamma \to \mu^+\mu^-$

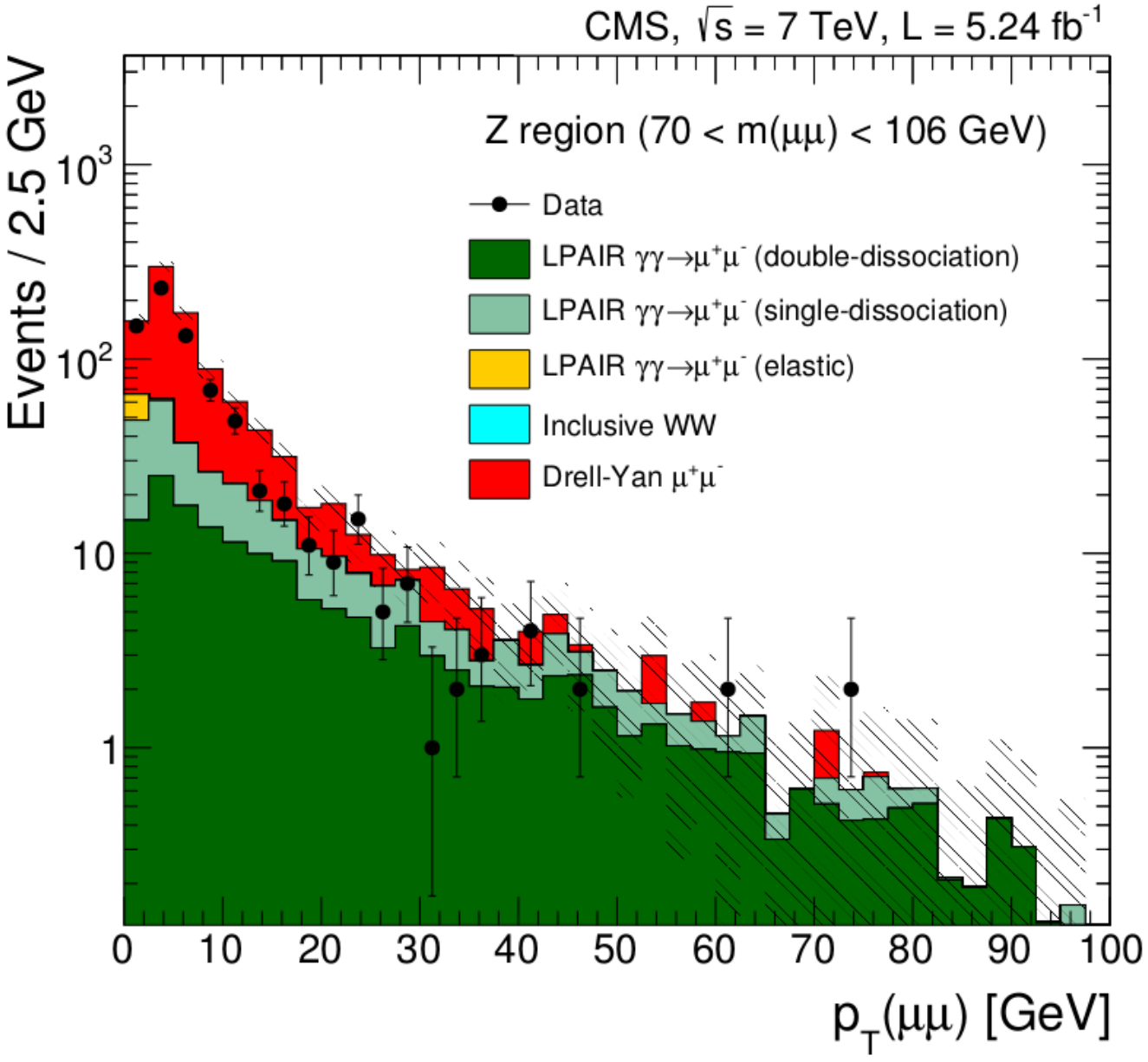

Efficiencies for $\gamma\gamma \to W^+W^-$

Selection step	Signal $\epsilon \times A$	Visible cross section (fb)	Events in data
Trigger and preselection	28.5%	1.1	9086
$m(\mu^{\pm}e^{\mp}) > 20\,\text{GeV}$	28.0%	1.1	8200
Muon ID and Electron ID	22.6%	0.9	1222
$\mu^{\pm}e^{\mp}$ vertex with zero extra tracks	13.7%	0.6	6
$p_T(\mu^{\pm}e^{\mp}) > 30\,\text{GeV}$	10.6%	0.4	2

Backgrounds for $\gamma\gamma \to W^+W^-$

Region	Background process	Data	Sum of backgrounds	$\gamma\gamma \to W^+W^-$ signal
1	Inclusive W^+W^-	43	46.2 ± 1.7	1.0
2	Inclusive Drell-Yan $\tau^+\tau^-$	182	256.7 ± 10.1	0.3
3	$\gamma\gamma \to \tau^+\tau^-$	4	2.6 ± 0.8	0.7

Systematic uncertainties for $\gamma\gamma \to W^+W^-$

	Signal uncertainty	Background uncertainty (events)
Trigger and lepton identification	4.2%	0.02
Luminosity	2.2%	0.005
Vertexing efficiency	1.0%	0.005
Exclusivity and pileup dependence	10.0%	0.05
Proton dissociation factor	16.3%	0.02

Missing E_T for $\gamma\gamma \to W^+W^-$

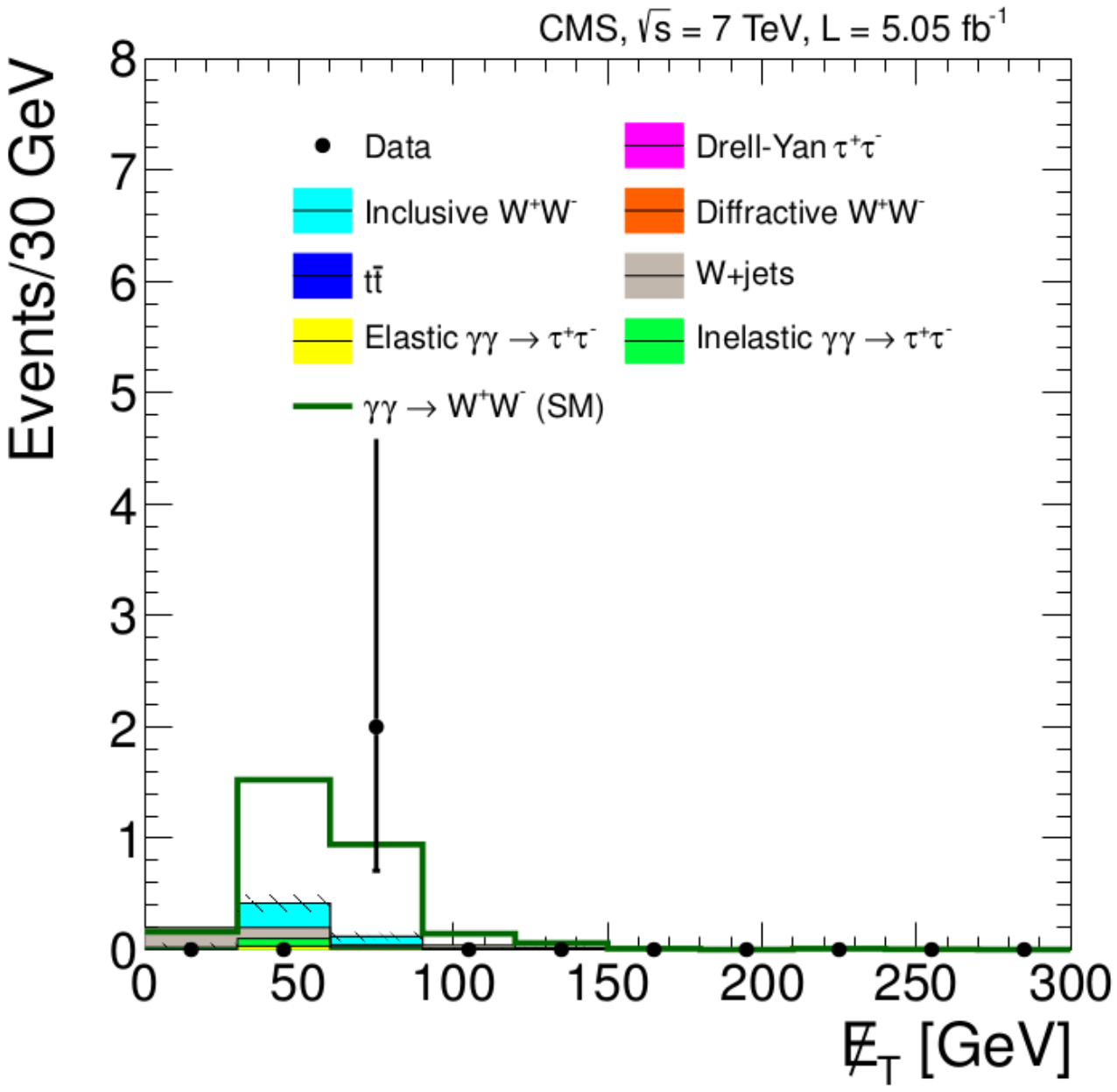

Efficiencies in aQGC

a_0^W/Λ^2	$[\mathrm{GeV}^{-2}]$	0	2×10^{-4}	-2×10^{-4}	7.5×10^{-6}	0
a_C^W/Λ^2	$[\mathrm{GeV}^{-2}]$	0	0	-8×10^{-4}	0	2.5×10^{-5}
Λ	[GeV]	—	500	500	No form factor	No form factor
Efficiency		$30.5 \pm 5.0\%$	$29.8 \pm 2.1\%$	$31.3 \pm 1.8\%$	$36.0 \pm 1.7\%$	$36.3 \pm 1.8\%$